AD-A049 846 STANFORD UNIV CALIF STANFORD ELECTRONICS LABS F/G 9/2
SEMI-ANNUAL STATUS REPORT NUMBER 132, 1 JANUARY THROUGH 30 JUNE--ETC(U)
JUN 77 N00014-75-C-0601
UNCLASSIFIED SU-SEL-77-037 NL

1 of 2
ADA049 846

STANFORD ELECTRONICS LABORATORIES

DEPARTMENT OF ELECTRICAL ENGINEERING
STANFORD UNIVERSITY · STANFORD, CA 94305

SEL-77-037

SEMI-ANNUAL STATUS REPORT NO. 132

1 January through 30 June 1977

This work was supported wholly by the
Joint Services Electronics Program
(U.S. Army, U.S. Navy, and U.S. Air Force)
Contract N00014-75-C-0601

Prepared by

Information Systems Laboratory
Digital Systems Laboratory
Integrated Circuits Laboratory
Solid-State Electronics Laboratory
Radioscience Laboratory
Institute for Plasma Research
Ginzton Laboratory

(14) SU-SEL-77-037

(6) SEMI-ANNUAL STATUS REPORT Number 132

1 January through 30 June 1977.

(11) 30 Jun 77 (12) 102p.

This work was supported wholly by the
Joint Services Electronics Program
(U.S. Army, U.S. Navy, and U.S. Air Force)
Contract (15) NØØØ14-75-C-Ø6Ø1

Prepared by

Information Systems Laboratory
Digital Systems Laboratory
Integrated Circuits Laboratory
Solid-State Electronics Laboratory
Radioscience Laboratory
Institute for Plasma Research
Ginzton Laboratory

J. D. Meindl, Director
Stanford Electronics Laboratories
Stanford University Stanford, California

332 400 4B

PERSONNEL

Faculty and Professional Research Staff

R. N. Bracewell
T. M. Cover
F. W. Crawford
R. W. Dutton
M. J. Flynn
M. Frankel
G. F. Franklin
A. C. Fraser-Smith
J. T. Gill
J. W. Goodman
R. M. Gray
S. E. Harris
M. E. Hellman
T. Kailath
I. Lindau
A. Macovski
E. J. McCluskey
J. D. Meindl
M. Morf
S. S. Owicki
G. L. Pearson
A. M. Peterson
W. E. Spicer
W. M. vanCleemput
O. G. Villard, Jr.
A. T. Waterman, Jr.
B. Widrow
J. F. Young

Student Research Staff

A. Abuel-Haija
D. Andelman
G. Aral
T. Bennett
N. Bhatnagar
D. M. Bubenik
N. Cot
J. Dobbins
N-H Duan
A. El Gamal
D. Estreich
R. D. Fleming
B. Friedlander
C. M. Garner
D. Hanson
A. Ho
A. Huang
J. Hupp
J. Iliffe
K. Jarett
K. Jew
R. Kahn
R. King
S-Y Kung
D. Lee
R. Lee
B. Lévy
J. Mandeville
J. Miller
J. H. Newton
J. Nickolls
W. Rogers
D. Rosenfeld
D. J. Rossetti
M. Salehi
S. Shah
A. L. Steinbach
K. Stevens
F. W. Terman
P. Thompson
J. van Campenhout
G. Verghese
E. Verriest
A. Vieira
A. von Bechtolsheim
S. Wakefield

CONTENTS

(cont on p vi)

CONTENTS (Cont)

ILLUSTRATIONS

TABLE

I. INFORMATION SYSTEMS

A. Project 6151. STATISTICAL DATA PROCESSING AND PATTERN RECOGNITION

Principal Investigator: T. M. Cover
Staff: R. King, A. El Gamal, W. Rogers, K. Jarret, J. van Campenhout, M. Salehi, N-H. Duan

1. Objective

The purpose of this project is to investigate problems of information processing and pattern recognition.

2. Current Status of Work

a. The Arbitrary Relationship between Probability of Error and Measurement Subset (J. van Campenhout)

Consider a two-class hypothesis-testing problem in which Ω is the set of possible features. Let $S \subseteq \Omega$ denote a feature subset and $P_e(S)$ denote the optimal Bayes risk (probability of error) incurred when the measurements S are used.

This research considers the possible values of $P_e(S)$ as a function of the feature subset S in a two-class problem with equal prior probabilities. All orderings of $P_e(S)$ and $S \subseteq \Omega$ satisfying the natural monotonicity condition $S' \subseteq S \Rightarrow P_e(S') \geq P_e(S)$ can occur. No other restrictions exist on $P_e(S)$, $0 < P_e(S) \leq 1/2$; therefore, the known result can be extended from the achievability of orderings to the achievability of numerically specified sequences.

During the course of the proof, a family of multivariate normal distributions capable of inducing any allowable numerically specified misclassification probabilities is observed. A paper has been submitted for publication.

b. Markov Channel Codes (K. Jarret)

The conjecture that first-order Markov encoding is sufficient to achieve any rate pair within the capacity region of a memoryless multiple-access channel with feedback has been disproved by counterexample.

The most general possible first-order Markov encoding, with four free parameters, was constructed for the binary erasure channel (x_1, x_2 binary, $y = x_1 + x_2$). An upper bound on $H(Y)$ was constructed and maximized over the code parameters. This maximum H was less than $R_1 + R_2$ for known achievable rate pairs. First-order Markov encoding, therefore, is not sufficiently rich to achieve capacity.

c. Multiple-Access Channels with Noisy Feedback (R. King)

Channel capacity can be increased when noiseless feedback is added to a multiple-access channel--a channel with two or more transmitters and one receiver. In a general communications network, however, feedback may not be noiseless but only statistically related to the channel output. Noisy feedback can be superior to noiseless feedback if the corrupted feedback is not a degraded form of the output. Total cooperation is often possible between two transmitters sending independent messages to one receiver even if the observed feedback is not a deterministic function of true output.

d. The Feedback Capacity of Degraded Broadcast Channels (A. El Gamal)

The capacity region remains unchanged if feedback is added to the physically degraded broadcast channel. This is consistent with Shannon's observation of the discrete memoryless channel with feedback. The result has been established both for discrete memoryless and continuous-amplitude gaussian channels.

e. The Capacity of a Class of Broadcast Channels (A. El Gamal)

The capacity region has been established for a class of broadcast channels $p(y,z|x)$ for which $I(X;Y) \geq I(X;Z)$ for all input distributions $p(x)$. This region resembles the capacity region of the broadcast channel with degraded message sets and extends the work on degraded broadcast channels.

f. The Resolution of an Apparent Paradox (J. Van Campenhout)

The peaking phenomenon of the Bayes recognition accuracy of pattern classifiers with unknown underlying statistics is being investigated. This effect is caused by improper comparisons of statistically incomparable models. A formalization of comparability has been introduced, and some of the results obtained in the literature are being analyzed in this context. A paper is in preparation.

B. Project 6240. OPTIMAL CODES WITH VARIABLE WEIGHT SYMBOLS

Principal Investigator: J. Gill
Staff: N. Cot

1. Objective

The objectives of this project are to determine procedures for producing optimal uniquely decipherable codes, using symbols of unequal costs, and to study the properties of optimal codes.

2. Current Status of Work

We have demonstrated that variable-length coding schemes can be applied to several fields other than communications. These include

(a) game theory where they are associated with the determination of optimal gambling strategies

(b) data allocation in storage and data retrieval [1] where their application is based on the relationship between double-chained trees and variable-length codes; a file can be organized as a double-chained tree in which keys correspond to variable-length code words

In (b), an optimal tree (or code) corresponds to a minimal average search time. If $0 < b_1 < b_2 < \ldots < b_t$ are the costs of the symbols of a code alphabet and if λ is determined by

$$\lambda^{-b_1} + \lambda^{-b_2} + \ldots + \lambda^{-b_t} = 1$$

then the converse to the source-coding theorem provides a lower bound on the average cost $\bar{c}$ of a code $\{w_1,\ldots,w_n\}$ with code-word probabilities $\{p_1,\ldots,p_n\}$,

$$\bar{c} \geq \frac{H(p_1, \ldots, p_n)}{\log_2 \lambda}$$

where $H(p_1,\ldots,p_n)$ is the entropy (in bits) of the probability distribution $p_1,\ldots,p_n$.

We have established an upper bound on the cost of optimal codes,

$$\bar{c} < \frac{H(p_1, \ldots, p_n)}{\log_2 \lambda + b_1 + \delta}$$

where $\delta \leq b_t$ is a quantity calculated from the costs $b_1,\ldots,b_t$. Using this upper bound, we can efficiently determine nearly optimal codes for unequal probabilities.

For equiprobable code words, a procedure [2] for producing optimal codes has been analyzed and shown to require $O(\log^t n)$ steps to produce optimal codes with n code words, and the cost of these code words was determined in Ref. 3. This procedure is being extended to nearly equiprobable code words.

References

1. L. Stanfel, "Optimal Trees for a Class of Information Retrieval Problems," Info. Stor. Retr., 9, 1973, pp. 43-59.

2. N. Cot, "The Complexity of the Variable-Length Encoding Problem," Sixth Southeastern Conference on Combinatorics, Graph Theory, and Computing, 1975.

3. N. Cot, "Cost of Optimal Prefix Codes," Johns Hopkins Conference on System Sciences, Apr 1977.

C. Project 6302. PROBLEMS IN CONTROL

Principal Investigator: G. F. Franklin
Staff: G. Aral, S. Shah

1. Objective

This study is concerned with design problems in automatic control systems, especially when model uncertainty is present.

2. Current Status of Work

Among various techniques for order reduction in linear constant systems, partial realization has the following disadvantages.

- Based on experimental sample data, the results are strongly dependent on the sampling rate.
- Because Markov-parameter partial realizations are high-frequency approximations, they are inappropriate for control purposes.

To overcome the first difficulty, the following approach is suggested. Instead of taking the first $2n$ Markov parameters (the sequence of impulse response), the sample points should cover several main time constants of the plant. One can take parameters spaced k periods apart so that

$$2nkT \approx 3\tau$$

where

n = order of realization

T = sample period of data

τ = main time constant of the plant

This is a partial realization of a sampling rate of kT which is often too slow.

Starting with the transfer function $H_kT(s)$, one of the same degree $[H_T(s)]$ can be constructed at a sampling rate of T so that the $(ik)^{th}$ Markov parameter coincides with the i^{th} Markov parameter of $H_{kT}(s)$. Unfortunately, the result is not unique. Among the multiplicity of solutions, however, we suggest taking the one with the slowest poles. An algorithm to calculate $H_T(s)$ from $H_{kT}(s)$ has been developed consisting of

- solving for the zeros of a polynomial
- calculating k^{th} roots of the zeros
- solving a set of $n-1$ linear equations

A corresponding method for the multivariable system, based on a series expansion of matrix expressions, gives rise to the difficulty of convergence. Currently, the multivariable algorithm converges only if the eigenvalues of the sparsely sampled realization satisfy

$$|\lambda - 1| < 1$$

In Fig. 1.1, the impulse responses of the plant

$$G(s) = \frac{1}{(z - 0.5)^3}$$

are compared to the *first-order partial realization based on Markov parameters* using a sparsing of 4 and the second-order partial realization using a sparsing of 2. The more preferred low-frequency modeling is achieved through the time moments of the plant, which are the coefficients of s in the power-series expansion of $H(s)$ about $s = 0$,

$$\mathfrak{M}_i = \frac{(-1)^i}{i!} \frac{d^i H(s)}{ds^i}\bigg|_{s=0} = \frac{(-1)^i}{i!} \int_0^\infty h(t)\, t^i\, dt = H(-F)^{-i-1} G$$

In discrete systems, the same expressions are often carried over to the z domain as

$$M_i = \frac{(-1)^i}{i!} \frac{d^i H(z)}{dz^i}\bigg|_{z=0} = H(-\Phi)^{-i-1} \Gamma$$

which does not determine a physically meaningful quantity.

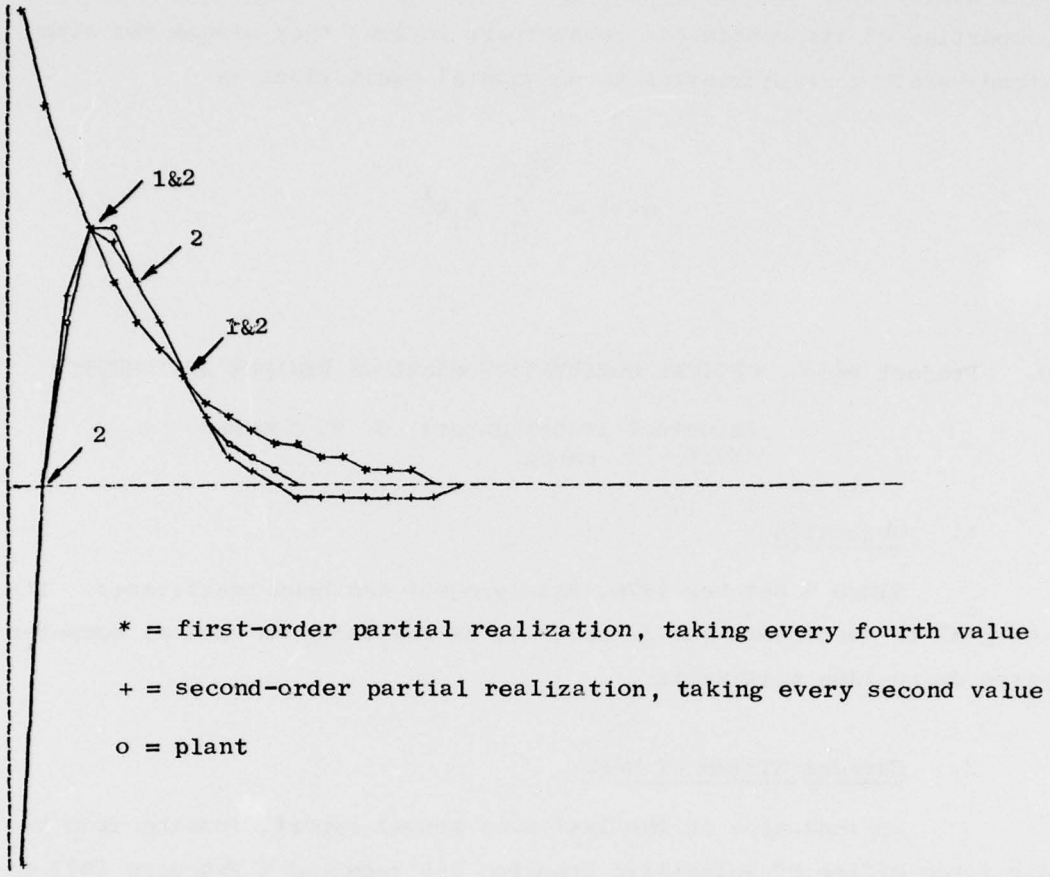

Fig. 1.1. IMPULSE RESPONSES VS FIRST- AND SECOND-ORDER REALIZATIONS. Arrows indicate sample instants where the impulse responses of the plant coincide with that of the model (*first order*, *second order*, or both are indicated by the numbers at the arrows).

A one-to-one physical relationship of discrete power-series expansion coefficients to those of the continuous system can be established if the expansion is performed about $z = 1$ which corresponds to $s = 0$ in the s-plane. The moments of a discrete plant, therefore, are defined as

$$M_i = \frac{(-T)^i}{i!} \frac{d^i H(z)}{dz^i}\bigg|_{z=1} = \frac{(-T)^i}{i!} \sum_{1}^{\infty} n(n+1) \ldots (n+i-1)\, h(nT) = H(\Phi - 1)^{-i-1}$$

Discrete partial realizations based on the above definitions have the properties of its continuous counterpart in that they assume the same steady-state characteristics to polynomial excitations as

$$u(t) = \sum_{i=0}^{2n-1} a_i t^i$$

D. Project 6418. OPTICAL COMPUTATION BASED ON RESIDUE ARITHMETIC

Principal Investigator: J. W. Goodman
Staff: A. Huang

1. Objective

Since 1 October 1976, this project has been reactivated. Its new goal is to explore the feasibility of realizing an optical computer based on residue arithmetic.

2. Current Status of Work

As indicated in the last semi-annual report, funding from the Air Force Office of Scientific Research was received 1 February 1977 to support this work. During the month of January, attention was focused on the decomposition of spatial maps into cascades of simpler maps to perform residue calculations. This decomposition allows a trade-off between the number of separate maps that must be selectable at a given point in the processor and the number of sequential maps required to accomplish a given mathematical operation.

The project was terminated on 31 January, and work was continued under the new AFOSR grant.

E. Project 6502. DATA-COMPRESSION TECHNIQUES AND APPLICATIONS

Principal Investigator: R. M. Gray
Staff: ---

1. Objective

The objective of this work is to develop nearly optimal data-compression algorithms having moderate complexity.

2. Current Status of Work

With the joint support of JSEP and AFOSR and during the past two years, approaches to trellis and tree-encoding data-compression systems for linear gaussian-source models have been studied via simulation. Such a system consists of a digital nonlinear filter as decoder and a matched-trellis (or tree) search algorithm such as a Viterbi algorithm as encoder.

Because the decoding filter determines the encoder structure, the design of this system is based on the selection of a decoder. A natural (and not original) choice is to take the decoder of a good data-compression system (such as DPCM) and to replace the encoder by its matched-trellis search. An alternative new approach is the "fake process" wherein a filter is designed so that, when driven by a memoryless binary process, the output "looks like" the original source. Two approaches were developed for generating the fake process--one based on the Central Limit Theorem and the other on inverse-distribution coders.

Extensive simulations of these systems were conducted for gaussian memoryless, autoregressive, and moving-average sources, mean-squared-error distortion measures, and low-rate codes. The trellis codes outperformed the traditional DPCM technique by 1 to 2 dB for sources with memory and the traditional PCM by approximately 0.4 dB for memoryless sources.

F. Project 6601. INFORMATION THEORY AND INFORMATION PROCESSING

Principal Investigator: M. E. Hellman
Staff: R. Kahn, D. Andelman

1. Objective

The objective of this project is to investigate the relationships between information theory, information processing, and complexity theory.

2. Current Status of Work

Improved coding schemes have been developed for the wiretap channel with feedback. Satellitization schemes, similar to those used in coding for broadcast channels, generate achievable (R,d) curves as opposed to single (R,d) points. The convexity of these curves has been demonstrated numerically, and a proof is sought.

Generalizations of the wiretap channel with feedback have been developed. In one, for example, there are two competing receivers. The transmitter has a message, but neither receiver knows to whom it is intended. The transmitter sends some data, asks for feedback, then sends more data. The goal of each receiver is to ensure that it properly decodes all messages intended for it and, subject to that constraint, to learn as much as possible about messages intended for the other receiver. If the initial transmission does not indicate which is the intended receiver, there is hope that both receivers will provide correct feedback and that the transmitter can improve performance over that of the wiretap channel with feedback (which is equivalent to this model if the intended receiver is identified at the start). Somewhat surprisingly, it appears that it may not be possible to improve performance. Reasons for this are sought, and it is hoped that these results will aid in better understanding security-capacity trade-offs in communications.

G. Project 6701. THE RECURSIVE-FILTER ADAPTIVE LINE ENHANCER[†]

Principal Investigator: B. Widrow
Staff: P. Thompson

1. Objective

The adaptive line enhancer (ALE), consisting of a digital filter adapted to produce a minimum mean-square-error prediction of a future input, has proven to be a useful tool for detecting narrowband signals obscured by wideband noise and for estimating the spectral characteristics

[†]This work is supported partially by the United States Department of Energy.

of signals. Earlier research has provided a good understanding of the behavior of the ALE when the adaptive filter is constrained to an all-zero tapped-delay-line (TDL) configuration. It is widely recognized that a recursive filter, containing both poles and zeros, can perform better with a smaller number of parameters than an all-zero filter; however, procedures for adjusting the parameters of such a filter are not well established. The objective of this research, therefore, is to develop and analyze appropriate adaptation algorithms for a recursive-filter adaptive line enhancer. A key to achieving this objective will be to constrain the filter to a configuration appropriate for the line-enhancer application in which high "Q" resonances are desired. By exploiting this implicit prior knowledge of the optimal filter configuration, it will be possible to avoid many of the difficulties normally encountered with the adaptation of recursive filters.

2. Current Status of Work

A possible configuration for a recursive-filter adaptive line enhancer (Fig. 1.2a) is obtained from an all-zero ALE by attenuating the input and closing a feedback path around the adaptive TDL filter; this is based on the rationale that the enhanced-signal output constitutes a less noisy source of signal with which to drive the TDL filter than does the input. The poles and zeros of the resulting recursive filter are adjusted simultaneously by adapting the weights of the TDL filter in much the same way that they are adapted in an all-zero ALE. The selectable parameter α appearing in the input and feedback paths controls the degree to which the filter transfer function is influenced by its poles. With $\alpha = 0$, the feedback path is open and the poles play no role; with $\alpha = 1$, the input is cut off leaving only the natural modes which are dominated by pole locations. With $\alpha < 1$, the adaptive filter can produce the desired high "Q" resonances at the frequencies of narrowband inputs.

The system in Fig. 1.2a is best understood in terms of its input-to-error transfer function, written as

$$H(z) = 1 - \frac{(1 - \alpha)\, A(z)}{1 - \alpha\, A(z)} = \frac{1 - A(z)}{1 - \alpha\, A(z)} \qquad (1.1)$$

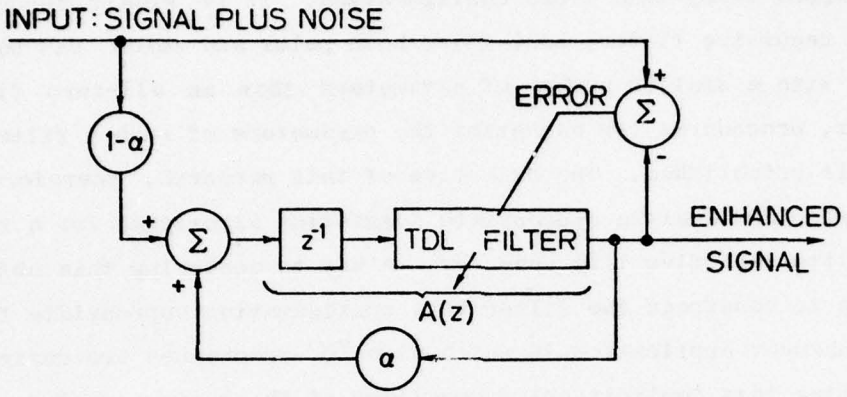

a. Block diagram

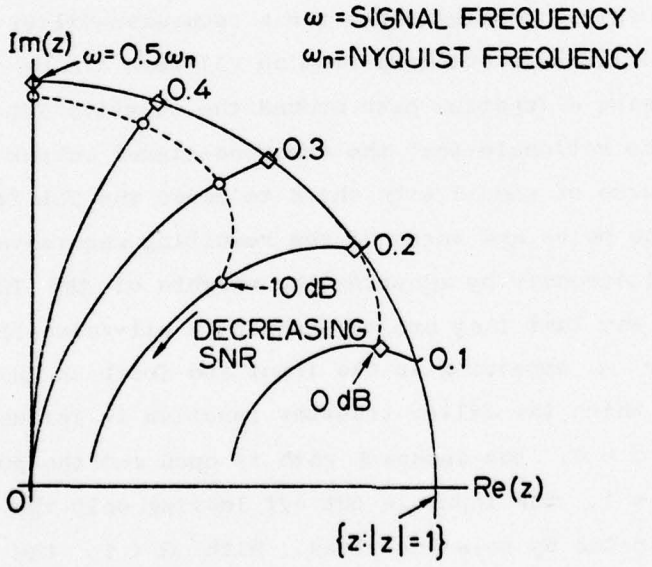

b. Loci of convergent zero locations for second-order case where $\alpha = 0.90$

Fig. 1.2. A RECURSIVE-FILTER ADAPTIVE LINE ENHANCER.

where

$$A(z) = a_1 z^{-1} + a_2 z^{-2} + \ldots + a_n z^{-n} \qquad (1.2)$$

Ideally, the error output should contain all of the noise and none of the signal because the enhanced-signal output would then consist of signal without noise. At convergence, therefore, the input-to-error transfer function $H(z)$ should approach zero gain at frequencies where signals occur and unit gain at all other frequencies. It follows that the zeros of $H(z)$ should approach the unit circle at angles corresponding to signal frequencies. The poles of $H(z)$ are kept "close" to the zeros if $\alpha \doteq 1$, thereby maintaining a gain of approximately 1 at frequencies away from those of the signal.

The actual convergent zero locations computed for the second-order ALE in Fig. 1.2a are plotted in Fig. 1.2b. The curves represent loci of zero locations for varying signal-to-noise ratios at several signal frequencies. It can be seen that, for sufficiently high SNRs, the zeros approach the unit circle at the desired frequencies; at lower SNRs, they converge to points well within the unit circle. It is also apparent that the system will perform much better at signal frequencies near half-Nyquist than at frequencies near zero or (by symmetry) near-Nyquist where the zero locations tend to be biased away from the signal frequencies. For larger α, the zeros would move closer to the unit circle for any given SNR.

An alternative configuration for a recursive ALE can be obtained by extending the above discussion concerning the desired form of $H(z)$. It can be argued that, in addition to having zeros near the unit circle at angles corresponding to signal frequencies, $H(z)$ should have poles at the same angles but with slightly smaller magnitudes to provide the desired sharp nulls. This implies that the input-to-error transfer function should be in the form of

$$H(z) = \frac{1 - A(z)}{1 - A(z/\rho)} = \frac{1 - a_1 z^{-1} - a_2 z^{-2} - \ldots - a_n z^{-n}}{1 - \rho a_1 z^{-1} - \rho^2 a_n z^{-n} - \ldots - \rho^n a_n z^{-n}} \qquad (1.3)$$

where ρ is a selectable parameter that controls the separation of poles and zeros. Figure 1.3a is a block diagram of a recursive ALE based on the transfer function in Eq. (1.3). This system is more complicated but appears to have superior qualities, as can be observed in Fig. 1.3b where

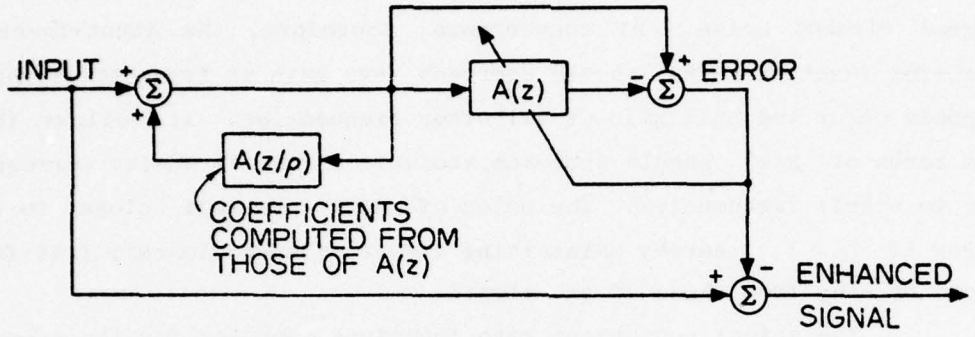

a. Block diagram

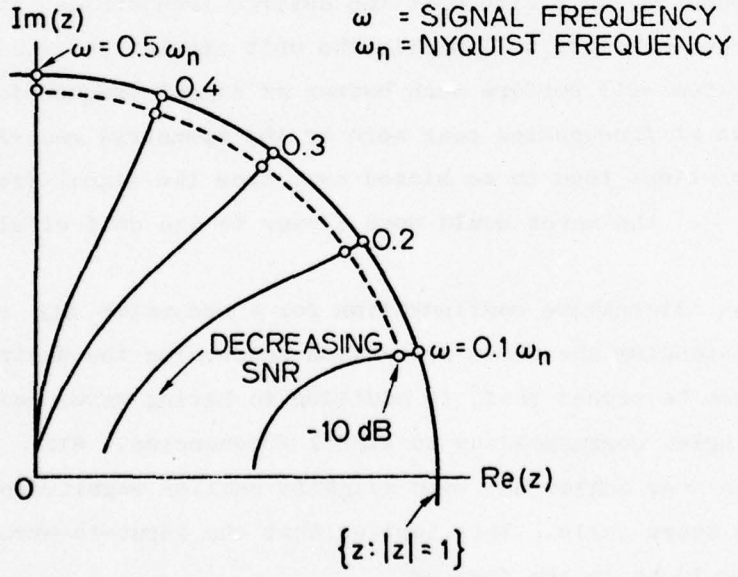

b. Loci of convergent zero locations for second-order case where $\rho = 0.95$

Fig. 1.3. AN ALTERNATIVE RECURSIVE-FILTER ADAPTIVE LINE ENHANCER.

the loci of convergent zero locations are plotted for a second-order ALE with this configuration. (We use $\rho = 0.95$ compared to $\alpha = 0.90$ in Fig. 1.2b to provide similar pole/zero separation in the radial direction.) Figures 1.2b and 1.3b indicate that the filter configuration associated with Eq. (1.3) will place its zeros more accurately at low signal frequencies and low SNRs than will that associated with Eq. (1.1). Simulation experiments confirm this result.

Both recursive-filter adaptive line enhancers promise to provide significant signal enhancement and accurate spectral estimates with a small number of adjustable parameters. Both have been simulated on a minicomputer and were found to converge to the predicted parameter values in a reasonable amount of time. Future work will be aimed at quantifying behavior and comparing performance to proven signal-processing techniques. Results will be extended to higher order filters and multiple sinusoidal signals and to signals with nonzero bandwidth and colored noise.

H. Project 6851. IMAGING OF GAMMA-RAY DISTRIBUTIONS

Principal Investigator: A. Macovski
Staff: A. L. Steinbach, D. Rosenfeld

1. Objective

The objectives of this work are to study the fundamental characteristics of a gamma-ray source distribution and to derive optimal methods for imaging such distributions. Because refractive effects do not exist at these energies, various attenuative masking structures are being investigated with respect to efficiency, resolution, depth delineation, and signal-to-noise ratio.

2. Current Status of Work

Work on this project has been terminated. Two dissertations have been completed--each describing alternate approaches to the imaging of gamma-ray distribution.

The first investigated zone-plate imaging systems. A complete deterministic analysis of the three-dimensional impulse response was made, and computer simulations served as the basis for the design of an optimal configuration.

The second focused on a modulated-aperture imaging system. Optimal codes were derived for the time modulation of the apertures, and computer simulations were made to illustrate the source-dependence of these codes. The stochastic nature of the imaging process was analyzed in detail.

I. Project 7050. STUDIES IN STATISTICAL SYSTEM THEORY

Principal Investigators: T. Kailath and M. Morf
Staff: J. Dobbins, D. Lee, B. Lévy, J. Nickolls, G. Verghese, E. Verriest, and A. Vieira

1. Objective

The purpose of this project is to study the basic problems in statistical system theory.

2. Current Status of Work

a. Realization of Time-Varying Impulse Responses (E. Verriest, T. Kailath)

Stationary systems have many properties, and the theory has been developed extensively. The known results obtained from stationary systems, therefore, should not be "lost" in the time-varying case, especially if the system is "close" to stationary. A measure of such closeness is defined through the $(\partial/\partial t+\partial/\partial s)$-operator, introduced earlier in our study of the distance of stochastic processes from stationarity. Using this operator, the time-varying impulse response can be expanded in a Taylor-like series around stationary functions. Based on a truncated series, a realization of an impulse response is obtained, consisting of time-invariant systems with time-varying coefficients belonging to a certain ring of functions. Conditions for observability/controllability can be determined in terms of eigenvalues of the invariant parts.

Further research will be directed toward a more abstract algebraic theory of time-varying systems--possibly connecting the former results with those obtained by Kamen.

b. Unification of Scattering Theory and Square-Root Approaches to Least-Squares Estimation (M. Morf, T. Kailath, G. Verghese, J. Dobbins)

Scattering theory has proven to be very powerful in generating such new least-squares estimation results as doubling formulas, change-of-initial-conditions formulas, and backward Markovian models. The square-root approach to estimation has also become important. A unifying framework to relate the results obtained from scattering theory and the square-root approach would be valuable. Not only could the scattering results be easily translated into numerically stable square-root algorithms, but the combination of highly visual scattering-theory techniques with the stochastic Gram-Schmidt processes underlying the square-root approach should facilitate the development of insight and new results. Some progress toward unification has been made.

Change of initial conditions and doubling formulas have been derived naturally in the square-root framework. Translating some scattering results to square-root form apparently requires "square-roots" of indefinite matrices. Although this can be accomplished through factorizations in the form of $M = A \Sigma A'$, where Σ is a signature matrix, stochastic interpretation of these factorizations remains in question (it could lead to "imaginary" random variables).

c. New Algebraic Methods for Two-Dimensional Systems Theory (B. Lévy, S-Y. Kung, M. Morf, T. Kailath)

To extend the results obtained from one-dimensional systems theory and one-dimensional data processing to higher dimensional problems (such as image processing, object reconstruction, and geophysical and meteorological data processing), it appears that new mathematical techniques must be developed.

We have studied the properties of rational matrix transfer functions depending on two variables. In addition, we have successfully extended the existing one-dimensional results obtained from extracting

the greatest common right divisor (GCRD) of two 2-D polynomial matrices, Sylvester resultants, and matrix fraction description (MFD) of 2-D rational matrices. We have used these results to define state-space controllability and observability in a manner consistent with the minimality of 2-D systems. It was found necessary to introduce such mathematical tools as "primitive factorizations" of 2-D polynomial matrices and some algebraic geometric concepts that appear to be new to systems theory and specific to multidimensional problems.

We have also developed computational techniques for the modeling of 2-D systems; these include a generalization of Levinson's algorithm for the recursive estimation of a 2-D stochastic process and a generalization of Lanczo's recursion for the fast Padé approximation of the 2-D transfer function, given its Markov parameters. These algorithms are related to the theory of 2-D orthogonal polynomials on the hyper-unit-circle or on the hyper-real-line.

Our results include extensions of maximum-entropy spectral estimation techniques to the 2-D case, 2-D spectral factorization methods, and new smoothing algorithms for 2-D stochastic processes. By noting the analogy among 2-D, integer, and differential-delay systems (all belonging to the class of systems over a principal ideal domain ring), we were able to obtain new realization methods and matrix-fraction descriptions for such systems.

d. System and Restricted-System Equivalence of Models Described by Polynomial Operators (T. Kailath, M. Morf, S-Y. Kung, B. Lévy, G. Verghese)

The concept of system equivalence was introduced by Rosenbrock to generalize the notion of system similarity to nonstate-space models (described by polynomial operators). The definition of equivalence is relatively simple; given two descriptions of the same physical system by two different observers, one would like to determine whether these descriptions are the same from a "coordinate free" point of view.

We have studied equivalence based on polynomial operators and state-space models. Earlier definitions of system equivalence have been related, and an alternative definition based on the construction of a complete information set for a given differential system has been

proposed. The canonical decomposition of the state-space model into controllable/observable parts can also be extended to polynomial systems.

In some cases, however, as when the transfer function of the system is not correct or when the polynomial matrices are not in a row (or column reduced), additional restrictions on system equivalence are required to ensure that the structure of the system at infinity is preserved. In this context, it appears that the theory of 2-D homogeneous polynomial matrices provides a convenient tool for the study of the structure of polynomial systems at infinity.

e. Model Fitting of Covariance Data (A. Vieira, T. Kailath)

If a finite segment of a covariance function is known, one can fit an all-pole (autoregressive) model to it. This modeling is useful for such purposes as prediction and control. It can be realized by solving the so-called Yule-Walker (or normal) equations. Because of their Toeplitz structure, these equations can be solved in a recursive and efficient manner (n^2 operations for an $n \times n$ matrix) by a Durbin-Levinson algorithm that can be recognized also as the Szego recursions for polynomials orthogonal on the unit circle. We have established the relationship of this algorithm to some synthesis procedures in the network theory of Brune and Darlington, wherein elementary sections of a transfer function are factored out. This factorization procedure can be applied to a class of transfer functions larger than all-pole models. Based on this knowledge, we were able to develop an algorithm for the fitting of a pole-zero model to covariance data. Details are still being investigated.

f. Ladder Structure for Least-Squares Estimation (M. Morf, A. Vieira, D. Lee, T. Kailath)

We have extended our earlier ladder structure to the so-called "nonwindowed" or covariance method of least-squares estimation. Using our previous results, we were able to handle the case where data values before the known ones are considered to be zero (prewindowing). Although this has produced excellent results, windowing of the data is

often considered undesirable. As a result, we have developed a ladder structure that works within the given data (no windowing) and is only slightly more complex than the prewindowing method. A trade-off between complexity and better results must be decided by the user.

g. Extended Interpretations of Ordered-Reduction Algorithms (G. Verghese, T. Kailath)

An algorithm developed by Dewilde to obtain the Smith-McMillan structure of a rational matrix at any frequency from its Laurent expansion at that frequency has been observed to be identical to the "structure" algorithm of Silverman. The structure algorithm is used in many problems in system theory but lacks the Smith-McMillan interpretation because, in most of these problems (such as system inversion), the frequency of interest is infinity and the Smith-McMillan form applies only to finite frequencies. The extension to infinite frequencies, however, is straightforward and necessary.

Based on this insight, we have been able to obtain a unified understanding of problems as diverse as inversion, realization from polar expansions, the role of infinite-decoupling zeros, and the asymptotic behavior of multivariable root loci.

h. A Scattering Framework for Estimation (B. Friedlander, T. Kailath, G. Verghese)

Our earlier study of a scattering model for estimation focused on the medium properties. Recently, we have identified the propagating waves in the medium, which are the smoothed state estimate and an adjoint state. As a result, we now have simple pictorial ways of visualizing, deriving, and organizing the major known smoothing formulas, including those for the effect of altered a-priori data on the estimates.

i. Square-Root Algorithms for Parallel Processing (M. Morf, J. Dobbins, T. Kailath)

We have developed a family of algorithms to process data in parallel for least-squares estimation problems. In a preliminary stage, data segments from disjoint time intervals can be processed

independently, and a compact set of information is then communicated between processors to yield the overall optimal estimates. All computations are performed in square-root form, and algorithms have been developed for both filtering and smoothing. In the preliminary processing stage, filters are independently initialized in each interval so that Chandrasekhar-type algorithms offer computational reductions even if the models are only piecewise constant. Thus far, algorithms have been developed only for the known model. Work is still in progress for the case where only covariance information concerning the observations is known.

II. DIGITAL SYSTEMS

A. Project 6961. DESCRIPTION LANGUAGES AND DESIGN FOR GENERAL-PURPOSE COMPUTER ARCHITECTURES

Principal Investigators: M. J. Flynn,
W. M. vanCleemput
Staff: T. Bennett, D. Hanson, J. Hupp, R. Lee,
K. Stevens, S. Wakefield, J. Iliffe,
A. von Bechtolsheim

1. Objective

The purposes of this study are to develop description languages to describe computer architectures and to establish a basis for understanding the limits of computer-architecture design (to determine the fastest speed for the execution of a program).

2. Current Status of Work

a. The SPRINT Printed-Circuit Design System
(W. M. vanCleemput, K. Stevens, T. Bennett, J. Hupp)

The objective of this system is to develop an interactive computer-assisted design of printed circuit boards. The SPRINT system allows for the manual placement of critical components and for automatic placement of such other components as 14- and 16-pin dual in-line packages. The interconnection routing module manually routes critical connections and automatically routes noncritical connections. The current system is limited to two signal layers; however, extension to multilayer boards is planned.

The input to SPRINT is called the Structural Description Language (SDL). In the future, the SDL will also be used as input to a logic simulator, a fault test-generation/simulation system, and automatic logic diagram generation.

SPRINT is implemented in MORTRAN and FORTRAN IV on the IBM 370 at SLAC and makes use of the Tektronix 4013 terminal. The SDL compiler is implemented in SPITBOL and SNOBOL dialect. The output is in the form of a plot from which the artwork must be generated manually.

b. Computer-Aided Layout of Large-Scale Integrated Circuits (W. M. vanCleemput, E. Slutz, W. Marti)

Although several systems exist for the automated layout of LSI circuitry, none obtains a layout comparable to one designed manually. The objective of this project is to develop and implement a system that uses algorithmic approaches in which certain decisions are the responsibility of the designer. It is expected that this system will reduce design time considerably at no expense of excessive silicon area. It will also be able to make use of hierarchical features if specified.

c. Interactive System for Design Capture (W. M. vanCleemput, A. von Bechtolsheim, B. Wong)

In the current design system, all input is in the form of the SDL. Because designers often prefer to use schematic diagrams to perform their tasks, a system is being designed that will take as its input a schematic drawing from an interactive graphics terminal and will output an SDL description for further processing by the various design-automation programs.

d. Bounds for Maximal Parallelism (R. Lee, M. J. Flynn)

This is a study of the performance limits of a single program executed on a large number of identical processors operating in parallel in an MIMD (multiple instruction multiple data) organization. Even with the rapidly decreasing cost of LSI microprocessors, it is not economically feasible to consider vast numbers of processors within the computer architecture to speed up a computation at the expense of component-processor efficiency. Some "acceptable" level of efficiency must be obtained. We must determine the overall speedup magnitude that can be expected by increasing the number of processors when the problems of control and communication that accompany the cooperation and competition between these processors are ignored.

We first defined a general model of computation on a p-parallel processor by distinguishing between logical parallelism (p* processors) inherent in a computation and physical parallelism (p processors) available in the computer organization. We then determined such

performance measures as execution time, speedup, efficiency, and the space-time product so as to evaluate the performance improvements (if any) of p-parallel processor systems compared to uniprocessor systems. The results obtained indicated that, generally, performance depends on both computer architecture and computation.

We then derived necessary and sufficient conditions for the maximum attainable speedup of a p-parallel processor to be $S_p \leq \min (p/\ln p, p^*/\ln p^*)$. This bound has never before been analytically established.

In addition, if there are always sufficient processors ($p \geq p^*$), conditions can be derived under which the maximum attainable speedup of a computation is $p^*/\ln p^*$, maximum efficiency is $1/\ln p^*$, minimum execution time is $T_1 \times \ln p^*/p^*$, and the minimum space-time product is $T_1 \times \ln p^*$ (where T_1 is the execution time of the computation of a uniprocessor). The empirical speedups obtained for a large number of different computations indicated that 80 percent of all programs examined satisfied these conditions and had maximum speedups of less than $p^*/\ln p^*$.

e. Parallel Information Processing in Biological Systems (S. Wakefield, M. J. Flynn)

The interconnections and types of synapses between the units of a neural subsystem (such as the stomatogastric ganglion of the lobster) have been determined by biologists, as have the stereotyped motor patterns that it produces; however, the exact mechanism and the sequence and duration bounds of impulse bursts that underlie the production of the coordinated muscle-activation patterns are unknown. Such a mechanism would be analogous to the switching network responsible for the traversal of states in a digital sequential circuit. Because of this analogy, this and similar biological information-processing subsystems are being investigated. In addition, speed, power requirements, size, information capacity, and other characteristics of individual neurons are being compared to those of electronic information-processing components.

f. Interpretive Machines (J. K. Iliffe, M. J. Flynn)

The motivation of this work is to achieve language implementations that are more effective in some measure of translation, execution, or response to the user than could otherwise be obtained. The implied comparison is to the established technique of compiling a code into a fixed general-purpose machine prior to execution. Although substantial benefits can be expected from microprogramming, it does not represent the best approach to design when such contributing factors as wide performance range, multiple source languages, and stringent security requirements must be satisfied. An alternative is to combine interpretation and a primitive instruction set and to provide security at the "microprogram" level.

B. Project 7151. COMPUTER ARCHITECTURE

Principal Investigators: E. J. McCluskey,
S. S. Owicki
Staff: D. J. Rossetti, F. W. Terman

1. Objective

The objective of this study is to gain new insight into computer architecture and operating systems. We intend to design a small operating system and to verify its correctness. A second goal is to develop new methods to evaluate system performance and to use the results obtained for better system design.

2. Current Status of Work

The basic methods for designing and verifying the correctness of concurrent programs have been analyzed. The design of a probably correct operating system is under way, and the high-level description is nearing completion.

The second direction of this project is focused on the evaluation of various computer architectures. Two methods that are very helpful in measuring performance are under study--a highly accurate modeling technique and monitoring systems.

A set of trace programs has been developed to measure microprocessor performance and to produce unique information concerning the programming ease of various microprocessors. The tracing is highly powerful (it can record interrupts and I/O behavior) and almost transparent (external hardware reduces significantly the amount of perturbation introduced by the tracer).

The investigation of interleaved memory is being extended to the effects of request ordering and to the most efficient ordering. A new model has been developed to evaluate the performance of gracefully degradable multiprocessor systems, based on such measures as availability, processing power, and proportion of time in the degraded mode. The best trade-off between computing power and availability or between hardware vs software fault detection can also be determined.

a. Verifying Concurrent Programs with Shared-Data Classes (S. S. Owicki)

Monitors are a valuable tool for organizing operations on shared data in concurrent programs. The mutually exclusive procedure calls provided by monitors, however, are sometimes overly restrictive. Such applications can be programmed using shared classes which do not enforce mutual exclusion. In one method for verifying parallel programs containing shared classes [1], one proves that each class procedure performs correctly when executed by itself and that simultaneous execution of other class procedures cannot interfere with its correct operation. After a class has been verified, calls to its procedures can be considered uninterruptible actions; this simplifies the proof of higher level program components. Proof rules for classes and procedure calls are presented in Hoare's axiomatic style. Several examples have been verified, including two versions of the readers and writers problem and a dynamic resource allocator.

b. Computer System Measurement (D. J. Rossetti)

Performance measurements have been divided into three areas--large-scale processor instruction tracing, microprocessor instruction tracing, and characterization of large-scale input/output environments.

The large-scale processor instruction-tracing facility is complete [2]. It is providing data for various studies of computer performance, architecture, and operating systems.

Microprocessor tracing is based on a hybrid hardware/software scheme to collect instruction frequency-distribution statistics for microprocessor-application programs. Some of its major characteristics are that it

- is independent of the program being traced
- traces bursts of instructions at a sample rate determined by the user
- causes minimal perturbation because tracing is assisted by the hardware

A third area of work is the gathering of sufficient data to characterize the input/output environment of large systems. We are in the process of obtaining complete I/O trace information for use in the architecture of novel storage systems involving new addressing schemes, technologies, and system structures. Four real-world environments are being measured, plus a variety of operating systems, processors, and I/O configurations.

c. Memory Interleaving (F. W. Terman)

A series of models of interleaved memory systems has been investigated by trace-driven simulations. The basic model extends the one developed by Burnett and Coffman [3] to the architecture of the IBM 360/370 with its variable-length instructions and operands [4]. It also includes multibyte transfers per memory access. Variations of the basic simulation model allow the study of the effects of channel interference, data-request reordering, and data-queue emptying at interrupts. The simulation model has been extended to include the effects of more than one processor accessing the same memory.

Memory requests for the simulations are obtained from two sets of instruction-by-instruction trace records. The first set traces the problem state component of typical programs running on the IBM 360/

370. The second set traces samples of the activity of the CPU, including supervisor and problem states.

Preliminary results indicate that, for high degrees of interleaving and large memory transfer widths (16-way interleaving and 16 bytes transferred per memory access), considerable improvement in effective memory bandwidth has been achieved by the presence of the additional processors; typical values are a $\sqrt{2}$ improvement in effective bandwidth for two processors and a factor of 2 improvement for four processors. For low degrees of interleaving and small memory transfer widths (four-way interleaving and four bytes transferred per memory access), the additional processors reduce the effective memory bandwidth because they interfere with each other in the fetching of instructions. Fewer instructions are fetched; therefore, fewer instructions are decoded and a smaller number of operand requests are generated per memory cycle.

The simulation studies have produced some interesting information concerning IBM 360/370 programs. For example, the average instruction length is 3.5 bytes, the average number of operand bytes required per instruction executed is 2.5, and 2/3 of these operand bytes are fetched with the remaining 1/3 being stored.

Current work is directed toward obtaining a better understanding of the mechanisms producing the effects observed from the various simulation models. A detailed comparison is also being made between the results from the simulation models and the various theoretical studies in the literature.

References

1. S. S. Owicki, "Verifying Concurrent Programs with Shared Data Classes," Tech. Rept. No. 147, Digital Systems Laboratory, Stanford University, Stanford, Calif., Aug 1977.

2. D. J. Rossetti and T. H. Bredt, "The Design and Implementation of an Operating System Tracer," Tech. Note No. 97, Digital Systems Laboratory, Stanford University, Stanford, Calif., 1977.

3. G. J. Burnett and E. G. Coffman, Jr., "A Study of Interleaved Memory Systems," Proc., AFIPS 1970 SJCC, 36, AFIPS Press, Montvale, New Jersey, 1970, pp. 467-474.

4. F. W. Terman, "A Study of Interleaved Memory Systems by Trace Driven Simulation," Proc. of Symp. on the Simulation of Computer Systems, 1976, pp. 3-9.

III. INTEGRATED CIRCUITS

A. Project 5012. IC PROCESS DESIGN AND COMPUTER MULTILAYER SEMICONDUCTOR DEVICE ANALYSIS

Principal Investigator: R. W. Dutton
Staff: D. B. Estreich

1. Objectives

Computer methods were developed to predict impurity profiles after processing, and physical parameters related to impurity diffusion were calculated.

Improved models will be developed for the prediction and simulation of the behavior of multilayer semiconductor devices based on layout and device-processing history.

2. Current Status of Work

The progress of integrated-circuit design has been toward higher density. The merging of elementary devices to form new semiconductor structures has been one method to achieve higher density. A good example of this approach is integrated injection logic (I^2L) which merges a lateral PNP with an inverse-operated vertical NPN to form a functional logic gate.

Reducing active device dimensions is another method for increasing integrated-circuit density. In some cases, undesired parasitics exist within an integrated-circuit structure, and scaling down often enhances the undesirable features of these devices. The best example may be the parasitic NPN and lateral PNP transistors inherent in standard CMOS integrated circuits. These transistors can lead to a latch-up failure mode (a four-layer p-n-p-n structure that regenerates into a high-current low-voltage state). A typical solution to reducing latch-up has been to increase the lateral dimensions of the layout; however, this decreases circuit density.

The purpose of this research is to (1) achieve greater understanding of the physics of the latch-up failure mode and to quantify the material and layout parameters that control latch-up in an integrated

circuit and (2) develop techniques and procedures to analyze and predict IC latch-up susceptibility from knowledge of the doping levels and circuit layout.

An important aspect of this research is to develop methods to identify potential latch-up paths. This requires knowledge of the circuit layout, including bias supply-contact locations, MOS source locations, and the design of the P-well region. Using this information plus substrate resistivity and the P-well impurity profile, a computer solution to Poisson's equation can be used to map the potential distribution in the bulk regions so as to identify the latch-up path (there may be more than one in some layouts). Measurement procedures are also being investigated for locating the latch-up path, using thermal methods.

After the latch-up path has been identified, computer programs based on Gummel's algorithm will be used to compute the current gains in the parasitic vertical NPN and lateral PNP transistors. This requires information concerning the impurity profiles, potential across the base of the lateral PNP, and bulk minority-carrier lifetimes. From the calculated current gains of the two parasitic transistors, latch-up susceptibility can be predicted--the critical condition for the initiation of latch-up is that the product of the NPN and PNP current gains must become unity.

Special test structures have been developed to isolate the geometrical factors, impurity profiles, and carrier lifetimes and to study their influence on latch-up.

The above methods and computational tools should be applicable to the latch-up analysis of any junction-isolated IC. This work should also be useful in considering the radiation effects in CMOS integrated circuits.

IV. SOLID STATE

A. Project 5111. TRANSPORT PROPERTIES OF $Al_xGa_{1-x}As$, $Al_xGa_{1-x}Sb$, AND $In_xGa_{1-x}As$ SINGLE CRYSTALS

Principal Investigator: G. L. Pearson
Staff: K. Jew

1. Objective

The purpose of this project is a systematic study of the transport of free carriers in these ternary systems. The electronic parameters are free carrier mobility, resistivity, minority-carrier diffusion length, activation energy, and trap energy levels. The distribution coefficients of selected doping impurities as a function of x are significant growth parameters. The results obtained should prove useful in the design of photoluminescent devices, injection lasers, solar cells, infrared detectors, and bulk-effect microwave devices.

2. Current Status of Work

A series of (p)$Al_xGa_{1-x}As$ crystals with compositions throughout the $0.0 < x < 1.0$ range was grown on (100)-oriented GaAs substrates, based on liquid-phase epitaxial techniques. Epitaxial layers grown on semiinsulating GaAs:Cr substrates were used for Hall-effect measurements. PN junction diodes made from (p)$Al_xGa_{1-x}As$ layers grown on (n^+)GaAs:Te substrates were used for measurements of capacitance voltage, current voltage, and length of minority-carrier diffusion.

All of the crystals were prepared by the same procedure. Before each growth, the gallium melt was baked out for 12 hr in flowing H_2 at 800°C. After bakeout, the dopant, GaAs source, Al, and GaAs substrates were loaded into the growth system. The p-type dopant was Ge having an atomic concentration of 0.5 percent in the melt. The amount of Al was varied to produce a range of ternary compositions. The crystals were grown in the temperature interval of 800° to 780°C and at a cooling rate of 0.2°C/min. The crystal compositions of the $Al_xGa_{1-x}As$ layers were measured through electron-probe microanalysis, and their Al distribution coefficient and growth rate were obtained.

Hall measurements of the (p)$Al_xGa_{1-x}As$:Ge crystals were made using the Van der Pauw technique. Carrier concentration, mobility, and resistivity were measured at 77° to 300°K.

Variation of the hole concentration at 300°K as a function of Al composition x is plotted in Fig. 4.1. The crystals were grown from melts containing 0.5 atomic percent Ge, and the effect of increasing Al content on dopant incorporation can be observed. The carrier concentration for GaAs at $x = 0.0$ is $\approx 10^{18}$ cm^{-3} which decreases exponentially with increasing Al content x as

$$p = 8.6 \times 10^{17} \exp(-3.98x) \qquad (4.1)$$

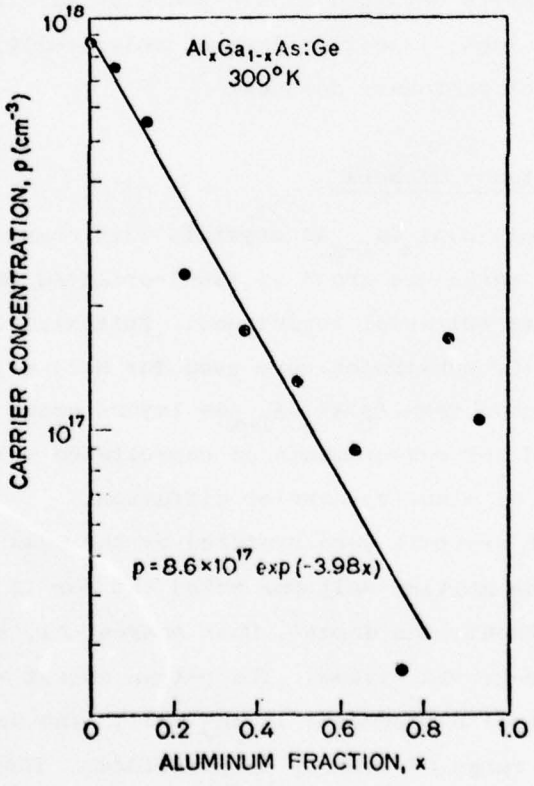

Fig. 4.1. CARRIER VS Al CONCENTRATION x IN LIQUID-PHASE EPITAXIALLY GROWN (p)$Al_xGa_{1-x}As$:Ge SINGLE CRYSTALS.

Because of the rapid decrease in hole concentration with an increase in x, samples with high Al content are closely compensated for by the background donor concentration, and there is some deviation from the general behavior described in Eq. (4.1).

The hole mobility at 300 °K as a function of Al composition x (Fig. 4.2) decreases from 170 cm^2/V-sec for GaAs to 40 cm^2/V-sec for AlAs. This decrease is caused by the increasing hole effective mass in the $Al_xGa_{1-x}As$ system as the Al fraction x is increased. For GaAs, the effective mass $m_p^* = 0.48\ m_o$ and, for AlAs, $m_p^* = 0.79\ m_o$. In $Al_xGa_{1-x}As$, it is assumed that the effective mass varies linearly with composition x so that

$$m_p^*(x) = (0.48 + 0.31x)\ m_o \qquad (4.2)$$

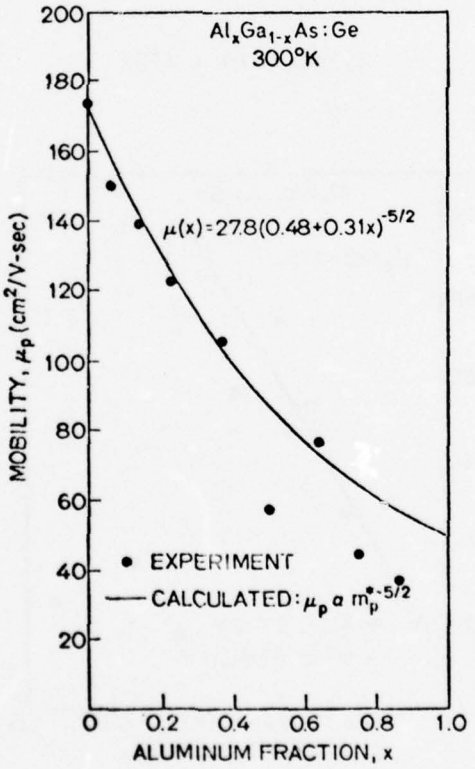

Fig. 4.2. HOLE MOBILITY VS Al CONCENTRATION x IN (p)Al_xGa_{1-x}As:Ge SINGLE CRYSTALS AT 300 °C.

Lattice scattering is dominant at room temperature and, for this scattering mechanism, mobility varies as $m_p^{*-5/2}$. Based on the assumed x dependence of m_p^*,

$$\mu_p(x) = A[(0.48 + 0.31x)\ m_o]^{-5/2} \qquad (4.3)$$

The proportionality constant was chosen to match the measured mobility of GaAs. The calculated result is plotted as the solid curve in Fig. 4.2 and is in good agreement with experimentally measured values.

Carrier concentration vs temperature generally varies as $p = p_o \exp(-E_a/kT)$, where the magnitude of p_o decreases with increasing Al composition x, as described above. The activation energy E_a (Fig. 4.3) becomes greater as Al composition x is increased and was obtained by curve fitting to the experimental data. In the $0.0 < x < 0.6$ range, activation energy increases from $\approx$20 to 120 MeV following the expression,

$$E_a(x) = 10 + 175x \qquad (4.4)$$

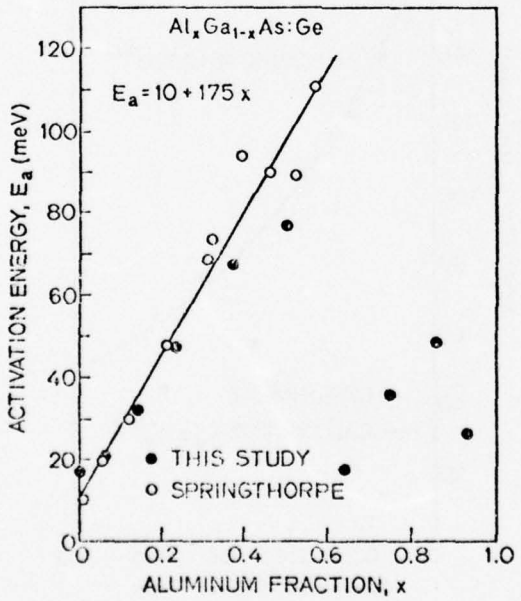

Fig. 4.3. ACTIVATION ENERGY OF Ge IN $Al_xGa_{1-x}As$ VS ALUMINUM COMPOSITION x.

Photoluminescence spectra of these crystals, measured in the direct band-gap range ($x < 0.37$) yield Ge energy levels in agreement with those obtained from Hall measurements. In crystals with high Al content ($x > 0.6$), there is wide deviation from Eq. (4.4) as a result of the close compensation between the Ge acceptors and background donors so that carrier concentration vs T does not vary with $p = p_o \exp(E_a/kT)$.

Variation of mobility with temperature is similar in all samples throughout the Al composition range ($0.0 < x < 1.0$); however, the magnitude of mobility generally decreases as the Al content x increases. A maximum μ_p occurs near 100°K. Below 100°K, μ_p decreases because of impurity scattering; above 100°K, it decreases as a result of lattice scattering and varies with temperature as $T^{-1.3}$.

A series of (p)$Al_xGa_{1-x}As$:Ge crystals grown on (n^+)GaAs:Te substrates was investigated. Diodes were fabricated from As grown wafers, after evaporating the metal contacts, by scribing and cleaving. The capacitance-voltage characteristics of these heterojunctions were measured to obtain the carrier concentrations in the crystal and in the built-in potential between the two heterojunction materials as a function of composition. The hole concentrations obtained by the C-V technique are similar to the results of the Hall measurements (Fig. 4.1). The current-voltage relationships of the diodes were used to analyze the transport of carriers across the (p)$Al_xGa_{1-x}As$-(n)GaAs interface as composition x was varied.

The electron-diffusion lengths in the (p)$Al_xGa_{1-x}As$ layers were obtained from the decay of the short-circuit current which was induced as the electron beam of an SEM was scanned across the cleaved edge of the p-n junction. This induced current decreases exponentially with distance X as $I = I_o \exp(-X/L_n)$, and decay is characterized by the diffusion length L_n. The electron diffusion lengths obtained are plotted in Fig. 4.4 as a function of Al composition x. At $x = 0$, $L_n \approx 6.3$ μm and decreases as the aluminum content is increased. Over most of the composition range x, $L_n \approx 1$ μm.

Studies of (p)$Al_xGa_{1-x}As$ at $x > 0.5$ are being continued. This work will then be extended to (n)$Al_xGa_{1-x}As$:Sn which will be characterized via Van der Pauw, photoluminescence, I-V, C-V, and scanning electron-microscope techniques.

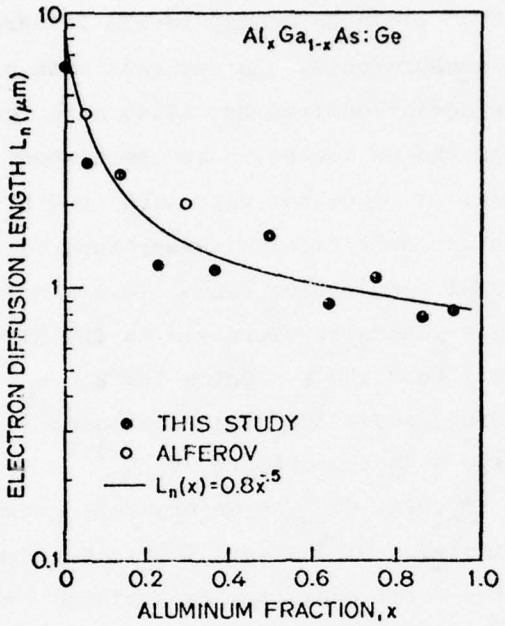

Fig. 4.4. ELECTRON DIFFUSION LENGTH VS Al CONCENTRATION x IN (p)$Al_xGa_{1-x}As$:Ge SINGLE CRYSTALS.

B. Project 5244. STUDIES OF HIGH-TRANSITION SUPERCONDUCTORS SUCH AS V_3Si AND Nb_3Sn AND DEPTH PROFILING OF $Al_xGa_{1-x}As$-GaAs HETEROJUNCTIONS

Principal Investigator: W. E. Spicer
Staff: I. Lindau, J. Miller, C. M. Garner

1. Objective

This project is involved in two areas of research. The first is to explore the electronic structures of type-II (hard) superconducting alloys, particularly the structure of Nb_3Sn, to determine such parameters as valence bandwidth which is important to the theoretical models of superconductors. Emphasis is directed toward the preparation of atomically clean Nb surfaces, followed by evaporation of Sn as an adlayer and annealing to form Nb_2Sn.

The second is to study the chemical interface between $Al_xGa_{1-x}As$ and GaAs in this heterojunction system, especially the chemical width of

the junction and surface morphology of the interface for various aluminum concentrations ($0.3 \leq \chi \leq 0.85$). The Schottky barrier Au-$A\ell_x Ga_{1-x}As$ interface is also examined.

2. Current Status of Work

a. Nb and the Oxidation of Nb (J. Miller, I. Lindau)

Because some of the highest T_c superconducting materials are Nb and Nb compounds, it is of interest to study the relationship of the electronic structure of these materials to their superconducting properties. With knowledge of the valence-band structure, various theoretical predictions associating these electronic and superconducting properties can also be tested. In addition, the oxidation properties of Nb are of value in such applications as microwave cavities and Josephson junctions.

In our experiment, the Nb samples were heat cleaned in an ultrahigh vacuum chamber with a base pressure of 4×10^{-11} torr. The Nb was heated by electron bombardment to within $\sim 200°$ of the melting point so as to remove all contaminants. Other cleaning techniques have been attempted unsuccessfully. Photoemission was applied on a He resonance lamp, using $h\nu$ = 21.2 and 40.8 eV lines simultaneously. The EDC is characterized by two d-band peaks; one has a large density of states near E_F and a shoulder 1.3 eV below E_F, and the other appears 2.8 eV below E_F. The measured valence-band width (4 eV) and general characteristics of the bands are in agreement with the bulk density of states calculated by Ho, Louie, Chelikowsky, and Cohen.[†]

Clean Nb was then exposed to small amounts of oxygen, and the growth of oxide peaks was monitored via UPS. With small exposures, a peak grows at 6.5 eV from E_F which is related to a chemisorbed stage. At larger exposures, a second peak appears at 7.3 eV from E_F and continues to increase; we associate this with the formation of a surface NbO_x (where $x = 2$ is a likely candidate). Higher exposures produce a third peak at 8.2 eV which grows until saturation; at this point, the

[†] Phys. Rev., B-15, 1977, p. 1755.

oxygen peak is similar to a sample left in air and known to form Nb_2O_5. Saturation exposure is associated with the formation of Nb_2O_5 at the surface. Having learned to prepare clean Nb, we now plan to study the Nb alloys because of their high superconducting transition temperatures.

b. Auger Profiling of III-V Heterojunctions and Schottky Barriers (C. M. Garner, C-Y Su, W. E. Spicer)

To produce III-V heterojunction devices, many growth techniques have been employed; however, the reproducibility of these devices was found to be poor. Because, in most III-V heterojunctions, the energy band gap will change in going from one side of the interface to the other, the electronic properties of a heterojunction depend on the variation of composition with distance through the interface. Similarly, Schottky-barrier heights often vary with sample-preparation techniques. To study these problems, we have used ion-milling Auger electron spectroscopy to analyze these samples for variation of composition with depth.

In studies of $Al_xGa_{1-x}As$-GaAs heterojunctions grown by liquid-phase epitaxy to produce the sharpest possible interface, it was found that samples grown at 800° and 750°C had interface widths of 120 and 100 Å, respectively. On the other hand, samples grown by LPE had interface widths of approximately 500 to 1500 Å; however, this technique developed fluctuations of Al concentration that caused a gradual instead of a sharp increase of photoresponse at the photon energies above the band gap of GaAs. Samples of vapor-phase epitaxy InP grown on InGaAsP were observed to have large concentrations of Ga in the VPE layer of InP, and this would alter the performance of the devices.

In studies of the Schottky barriers, chemical etching of the AlGaAs samples prior to deposition of Au was observed to increase the thickness of the oxide between the Au and $Al_xGa_{1-x}As$ and to change the barrier height. Analyses of Ag on heat-cleaned InP further revealed that a layer of In appeared on the surface of the Ag and that the In was in the form of an In oxide. A much smaller amount of P was also found on the surface of the Ag. This would drastically affect the device as a photoemitter because it would be necessary for the electrons to move through this In-oxide layer before escaping.

Our findings indicate that growth techniques can produce results other than those desired. Additional investigations of these systems and others are required to better understand the growth processes and the relationship of interface structure to the electronic properties.

V. RADIOSCIENCE

A. Project 3172. DIGITAL IMAGE PROCESSING

Principal Investigator: R. N. Bracewell
Staff: J. Mandeville

1. Objective

The purpose of this project was to investigate the applications of maximum-entropy reconstruction to the field of computerized tomography. There is a consensus that the benefits of iterative techniques are confined to circumstances where measurement coverage is deficient, for example, when projections are truncated or when the object is scanned over a limited angular extent. In situations other than these, a much faster convolution method produces images of acceptable quality. In addition, the trends toward faster scanning apparatus and larger arrays make relatively slow iterative processing undesirable unless the processing results in substantial improvements. Because of these faults, effort was concentrated on comparison of an error-tolerant maximum-entropy algorithm, ART, and the convolution method in deficient measurement situations.

2. Current Status of Work

Projection data sets corresponding to full coverage, truncated projection coverage, and limited angular coverage have been computed, and reconstructions from these data sets were then computed. The four reconstruction procedures were

- a maximum entropy algorithm
- additive ART
- multiplicative ART
- convolution

A major conclusion is that the maximum-entropy algorithm does not appreciably advance the state of the art of imaging in this field for the following reasons. First, it has been proved that multiplicative ART

converges to a maximum-entropy image. Not only does this relationship provide a convergent computer algorithm for maximum-entropy reconstruction, but it also suggests that the many empirical tests of multiplicative ART are indicative of the imaging performance of the maximum-entropy method. The reconstructions computed in this investigation confirm this qualitative equivalence between multiplicative ART and the maximum-entropy algorithm.

Second, it appears that maximum-entropy images suffer from many of the same artifacts present in images computed from deficient measurements by simpler and faster algorithms. This conclusion is confirmed by empirical tests and mathematical analyses of the equations defining maximum-entropy images.

Although maximum-entropy reconstruction has limited utility in computerized tomography, this technique offers advantages for such processing tasks as high-resolution spectral analysis and image reconstruction in radio astronomy. We have continued to develop the iterative strategy appropriate to these uses. Among the reasons favoring maximum-entropy analysis are less emphasis on processing speed, availability of fast algorithms based on FFT, and the nonnegativity constraint has more impact on data reduction than it does in computerized tomography.

B. Project 3606. RADIO ACOUSTIC SOUNDING SYSTEM

Principal Investigator: A. M. Peterson
Staff: M. S Frankel, N. Bhatnagar, A. Abuel-Haija

1. Objective

The purpose of this project is to study the capabilities and limitations of the Radio Acoustic Sounding System (RASS) as a means for measuring temperature profiles and winds in the lower atmosphere.

2. Current Status of Work

During this reporting period, important theoretical work has been completed, which delineates the effects of atmospheric turbulence and winds on the performance of the RASS. Contrary to our early

expectations and the predictions of other researchers, our study has demonstrated that a radio-acoustic system can operate at much higher frequencies than have previously been employed and still provide data to heights of greater than 1 km. The significance of this result is that, by increasing acoustic frequency, the size of the acoustic source (as well as the RASS) can be reduced. With a smaller source, it will be possible to build a transportable RASS to collect real-time atmospheric data at locations of the user's choice. These predictions have been experimentally verified [1] at an acoustic frequency of 1 kHz (440 MHz radio frequency).

This reporting period will conclude our work on the RASS which was initiated as a technique for real-time temperature profiling the first few kilometers of the lower troposphere [2]. The basic physics of the RASS is as follows.

The electromagnetic refractive index of air (above 30 MHz) in the lower troposphere is not exactly unity but is a function of pressure, temperature, and humidity. Because of its pressure dependence, this refractive index can be altered by a short pulse of sound from an acoustic source. An electromagnetic RF signal generated by a radar passes through the sound pulse and is scattered as a result of the induced refractive-index variations. This scattered signal is collected by a receiver and is processed to determine atmospheric temperature as a function of the acoustic-pulse position (range). In a static atmosphere, the received signal is maximized when a Bragg condition is established between the acoustic and electromagnetic signals. This occurs if the electromagnetic wavelength is twice the acoustic wavelength and results in an in-phase addition at the receiver of the electromagnetic signal scattered from successive acoustic wavefronts in the pulse.

A doppler radar measures the speed of the sound pulse. Because the speed of sound in air depends on its temperature, the temperature profile of the lower atmosphere can be obtained with the RASS [3]. Figure 5.1 illustrates the geometry of a bistatic RASS wherein the acoustic source is located between separated RF transmit and receive antennas. In a monostatic RASS, the antennas and acoustic source are located at the same point.

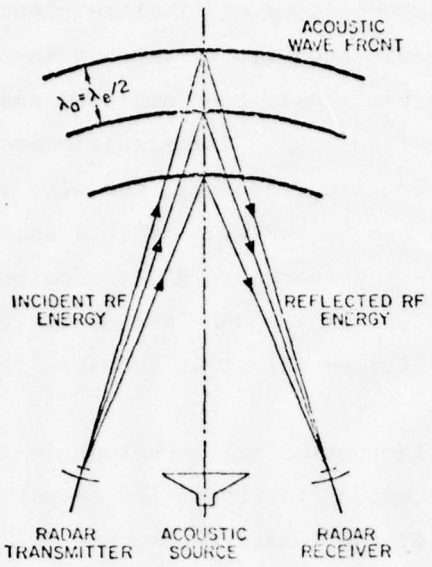

Fig. 5.1. REFLECTION OF ELECTROMAGNETIC ENERGY FROM AN ACOUSTIC PULSE FOR A RASS BISTATIC GEOMETRY.

In an early study at Stanford University [2], the reflection of electromagnetic energy from an acoustic pulse propagating vertically into the lower atmosphere was analyzed at a carrier frequency of 85 Hz. A static atmosphere (no turbulence or winds) was assumed, and no attempt was made to determine the feasibility of operating the RASS at acoustic frequencies higher than 85 Hz, which has the advantages of a smaller system and an increase in the resolution of the measured atmospheric parameters.

Recent work considers the interaction of electromagnetic and acoustic waves when the RASS is operated in a stochastic environment characterized by turbulence, winds, and mean-temperature gradients. These atmospheric parameters are important when evaluating RASS performance because they could affect the spatial coherency in and between the acoustic wavefronts of the transmitted acoustic pulse. This decrease in coherency would reduce the received signal levels.

An analysis of the effects of turbulence on the coherency of the acoustic wave reveals that the acoustic-wave amplitude at an altitude

x is damped by $\exp[-\langle |\psi_1(x,\bar{y}_\alpha)|^2 \rangle/2]$ because of complex-phase interference. In this damping factor, $\psi_1(x,\bar{y}_\alpha)$ is the first-order perturbation in the complex phase of the acoustic wave caused by turbulence.

These perturbations are small in the lower troposphere; consequently, for acoustic pulses with carrier frequencies below a few kilohertz propagating (under typical atmospheric conditions) to altitudes of a few kilometers, turbulence has little effect on the strength of the received radio signal. If altitude x of the acoustic pulse is much less than the coherence length of propagation x_c, the effect of turbulence on RASS performance is insignificant. This coherence length of propagation is

$$x_c = \left[\frac{54.8(1.833 - m_a)}{C_{no}^2 k_a^2 A^{5/3} x_o^{m_a}} \right]^{6/(11-6\, m_a)}$$

where m_a determines the acoustic refractive-index structure parameter in the presence of inhomogeneous turbulence, C_{no}^2 is the refractive-index structure parameter at altitude x_o, k_a is the acoustic wave number, and A is a proportionality constant that measures the outer scale of turbulence. It can be observed that the coherence length varies inversely with frequency and the strength of the turbulence. For example, consider a RASS operating at an acoustic frequency of $f_a = 2$ kHz and assume that $C_{no}^2 = 10^{-6}\ m^{-2/3}$, $x_o = 1$ m, $A = 2$, $m_a = 1.33$, and the velocity of sound $c_o = 340$ m/sec; the coherence length is then $x_c = 4 \times 10^7$ m. This value implies that the coherency of an acoustic wave is not affected by turbulence throughout the whole atmosphere when $f_a = 2$ kHz.

Quiescent atmospheric conditions (such as temperature gradients) cause the dispersion of the acoustic wavetrain. Under these circumstances, a match between electromagnetic and acoustic waves can be obtained by the use of a modified Bragg-scatter condition. This match depends on the temperature difference over the length of the acoustic wavetrain; however, typical temperature gradients in the lower atmosphere (on the order of -6.5°K/km) have a negligible effect on the received power of a RASS. The effect of vertical winds on the strength of the received radio signal can also be negligible.

Mean horizontal winds shift the focus of reflected electromagnetic energy from its origin, resulting in a decrease in received signal level when a monostatic RF system is used. Because the acoustic wavefronts act as large spherical reflectors, the principle of specular reflection, however, can be utilized in a bistatic radar geometry to measure this wind component remotely (in addition to atmospheric temperature profiles). In this RASS configuration, the radar antennas and acoustic sources are aligned in the wind direction--the transmit antenna upwind from the acoustic source and the receive antenna downwind. This technique has the potential of measuring horizontal wind velocities of magnitude up to a few tens of meters per second in the lower troposphere.

An experiment [1] consistent with our recent theoretical work was conducted at an acoustic frequency of 1 kHz (440 MHz RF). For periods when atmospheric winds were less than $\approx$4 m/sec, the radar antennas were placed diametrically opposite each other on a circle centered about the vertical axes of the acoustic array. A 6 m minimum spacing between these antennas was chosen so that the RF feedthrough (leakage) signal would be low enough to avoid saturation of the RF preamplifier. Because this separation is approximately one order of magnitude less than the minimum altitude from which data were obtained, this configuration is referred to as a monostatic RASS.

When winds were greater than $\approx$4 m/sec, it was necessary to configure the RASS as a bistatic radar. The radar antennas are aligned in the wind direction--the transmit antenna upwind from the acoustic source, and the receive antenna downwind. This configuration of antennas is necessary because horizontal winds move the focus of the acoustic wavefronts; however, by placing the antennas as indicated above, a "specular" reflection can be obtained when the focus of the acoustic wavefronts bisects the line drawn between the RF antennas. Under specular reflection conditions, signals comparable in magnitude to those calculated are obtained when the acoustic pulse is moved in the windward direction.

Three types of measurements were made during the experiment. First, data were collected during both windy and quiet conditions to determine the effects of winds on the maximum range of the system. During quiet conditions (winds less than a few m/sec), continuous echoes were

received to approximately 1 km, using a monostatic RASS. When winds exceeded a few m/sec, radar doppler signals from the acoustic pulse were limited to a 250 m altitude by wind shear near the ground. By orienting the radar antennas in the direction of the wind and moving the receive antenna downwind, however, the range at which echoes were received increased to 1 km. In addition to increasing the range over which doppler signals could be obtained, the bistatic RASS permitted us to determine horizontal wind speed and direction. These data were obtained by measuring the location of the radar antennas and the delay times between echoes received at each antenna location.

Second, ground-level temperature measurements were made with the RASS by Bragg-matching the RF and acoustic frequencies at low altitudes. These RASS temperatures were compared to ground measurements, and good agreement was observed.

Third, a measurement was made to understand the possible degradation of the acoustic wavefront coherency as the pulse propagates through regions of atmospheric turbulence. Results support our theoretical analysis that turbulence does not significantly degrade the performance of a high-frequency RASS over at least the first 300 m, even when very long acoustic pulses are transmitted.

References

1. M. S Frankel, N. J. F. Chang, and M. J. Sanders, "A High Frequency Radio Acoustic Sounder for Remote Measurement of Atmospheric Winds and Temperature," Bull. Amer. Meteorol. Soc., 1977.

2. J. M. Marshall, "A Radio Acoustic Sounding System for the Remote Measurement of Atmospheric Parameters," Sci. Rept. No. 39, Stanford Electronics Laboratories, Stanford University, Stanford, Calif., 1972.

3. M. S Frankel and A. M. Peterson, "Remote Temperature Profiling in the Lower Troposphere," Radio Science, 11, 1977, pp. 157-166.

C. Project 4214. INVESTIGATION OF UNDERSEA COMMUNICATION WITH ULF ELECTROMAGNETIC WAVES

Principal Investigator: O. G. Villard, Jr.
Staff: A. C. Fraser-Smith, D. M. Bubenik, A. Ho

1. Objective

The objective of this project is to investigate the propagation of ULF electromagnetic waves in the sea (frequencies less than 5 Hz) from undersea harmonic dipole sources, taking into account the effects caused by the presence of the ocean floor. This is an extension of earlier work [1-3] dealing only with an ocean of effectively infinite depth.

2. Current Status of Work

This project consists of (a) derivation of the mathematical expressions for the fields of harmonic dipole sources located in an ocean of finite depth, (b) evaluation of these expressions, and (c) analysis of the results. The progress in each of these stages is reported below.

a. Derivation of the Expressions

A complete set of expressions has been developed to determine the electromagnetic fields of the four principal elementary dipole sources (vertical magnetic and electric and horizontal magnetic and electric) in the presence of a layered conducting medium. Based on these formulas, the electromagnetic fields can be computed in any layer of a multilayered isotropic medium containing any of the above dipole sources. Both displacement and conduction currents may be considered, and there are no restrictions on frequency or source-receiver separation. To our knowledge, a set of expressions of comparable completeness and generality has not been available.

b. Evaluation

These expressions contain Sommerfeld integrals that, generally, cannot be evaluated in closed form. We evaluated the integrals numerically, therefore, using a technique developed in our Radioscience Laboratory [4].

c. Analysis of Results

The results are obtained in normalized form, with distances expressed in units of skin depth δ and with ocean-floor conductivity

normalized to that of sea water. This approach is economical because the frequency parameter is absorbed into the normalizing factors, and sea-water conductivity can be varied if desired by adjusting these factors.

To obtain a propagation path of significant length between each terminal and the sea-air/sea-floor interfaces but not excessively attenuating the fields in the water, both the transmitter and receiver were set at a depth of $\delta/2$ in an ocean one skin depth deep. Representative realistic conductivity contrast ratios ($\sigma_{floor}/\sigma_{sea}$ of 10^{-1} and 10^{-2}) were considered, and the horizontal source-receiver separation ρ ranged from 10^{-1} to 10^{2} δ, which corresponds to separations of 25 m to 25 km at 1 Hz.

From our analysis, we conclude that, for $\rho < 3\ \delta$, the underwater electromagnetic fields differ less than 3 dB from those produced by a dipole in an ocean of infinite extent. Thereafter, the computed fields rapidly become very much greater than the "infinite ocean" fields and exceed them by more than 600 dB at $\rho = 100\ \delta$. This indicates that other modes of signal propagation (such as the up-over-and-down mode above the surface and the down-under-and-up mode below the water/floor interface) must be the principal mechanisms that carry the signal to these large distances. We have developed a method for separating the contributions from these modes and the contribution from high-order more complex modes. Preliminary results indicate that the floor contribution is negligible relative to that of the surface mode for $\sigma_{floor}/\sigma_{sea} = 10^{-1}$ but forms a significant, although not major, portion of the net field for $\sigma_{floor}/\sigma_{sea} = 10^{-2}$.

Analysis of the large volume of data generated is continuing. More detailed results will be presented in a paper being prepared for publication.

References

1. J. R. Wait and H. H. Campbell, "The Fields of an Oscillating Magnetic Dipole Immersed in a Semi-Infinite Conducting Medium," J. Geophys. Res., 58, 1953, p. 167.

2. A. K. Sinha and P. K. Bhattacharya, "Vertical Magnetic Dipole Buried inside a Homogeneous Earth," Radio Science, 1, 1966, p. 379.

3. M. B. Kraichman, Handbook of Electromagnetic Propagation in Conducting Media, U.S. Government Printing Office, 1970.

4. D. M. Bubenik, "A Practical Method for the Numerical Evaluation of Sommerfeld Integrals," to be published in IEEE Trans. on Antennas and Propagation, Nov 1977.

D. Project 4504. TROPOSPHERIC RADIO PROPAGATION

Principal Investigator: A. T. Waterman
Staff: R. D. Fleming

1. Objective

The objective of this research is to investigate atmospheric parameters and phenomena in the lower troposphere based on radio propagation in the S- and K-bands. The goals are to

- measure wind velocity in the common volume of a transhorizon troposcatter propagation path by means of doppler techniques
- probe the structure of winds and turbulence in the lower troposphere under various conditions of atmospheric stability and instability

2. Current Status of Work

The equipment for wind measurement on a transhorizon propagation path has undergone a set of calibration checks to ensure accuracy. The plan of operation is to involve the simultaneous reception of 3 GHz CW signals, from a transmitter located 100 miles away (beyond line-of-sight), on each of two narrow beams aimed on either side of the great-circle bearing toward the transmitter by small amounts (1° or less). If a wind component is transverse to the path in the region of the common volume, it is anticipated that the signal received on one beam will be doppler shifted to higher frequencies and that the signal on the other will be shifted to lower frequencies. The magnitude of the doppler difference should be proportional to transverse-wind velocity. The two beams will be formed during data reduction because the receiving antenna is a sampling array that measures and stores on digital tape the

amplitudes and phases of the signal as received on 12 individual antennas. To obtain high azimuthal resolution, the antennas are arranged in a horizontal linear array.

The linear array to be used is an array of 12 4-ft parabolic dishes mounted on a 70-ft tower. Because the tower had been used in previous experiments in a vertical position, it was necessary to move it to a horizontal position. The balance of the equipment has been checked and is in operating condition.

Recent work has been directed toward calibrating the phase measurement system and organizing the computer-controlled data-gathering programs. The next step will be checking the system on a line-of-sight path before moving to the transhorizon configuration.

VI. PLASMA PHYSICS AND QUANTUM ELECTRONICS

A. Project 1337. GENERATION OF INTENSE MICROWAVE RADIATION

Principal Investigator: F. W. Crawford
Staff: ---

1. Objective

The aim of this project is to design and construct a high-power magnetron capable of producing ≈1-GW ≈1-μsec (≈1 kJ energy) pulses at ≈3 GHz.

2. Current Status of Work

Research conducted elsewhere [1,2] has resulted in an experimental cold-cathode relativistic magnetron capable of producing 1 to 2 GW pulses at 3 GHz, with pulse lengths on the order of tens of nanoseconds. During this reporting period, we have considered an improved version of this tube, using a hot cathode and better vacuum conditions, and incorporating the features of a high-power long-anode tube developed by Boot [3]. Because one of the intended applications of this tube is to the study of nonlinear parametric interactions in plasmas, support for the magnetron construction has been obtained from the Physics Division of the NSF. Our preliminary design for the power supply of the tube has been submitted for technical discussion and bids to three manufacturers.

References

1. T. J. Orzechowski and G. Bekefi, Phys. Fluids, 19, 1976, p. 43.
2. G. Bekefi and T. J. Orzechowski, Phys. Rev. Lett., 37, 1976, p. 379.
3. H. A. H. Boot, H. Foster, and S. A. Self, Proc. IEE, 105B (Suppl. 10), 1958, p. 419.

B. Ginzton Laboratory. TWO-PHOTON RESONANTLY PUMPED IR UP-CONVERTERS

Principal Investigators: S. E. Harris, J. F. Young
Staff: J. H. Newton

1. Objective

The goals of this project are the development and extension of efficient IR up-conversion techniques in metal vapors, particularly image up-conversion.

2. Current Status of Work

We have demonstrated the up-conversion of 2.9 μm IR images to 4550 Å in Cs vapor. A power efficiency of 20 percent, with over 1000 resolvable spots, was achieved using a pump power of only 8 kW focused in an area of 0.1 cm^2. The Cs cell had an active length of 0.2 cm and was operated at a density of 1.4×10^{17}/cc. The pumping laser, Nd:lanthanum-berylate, has a natural two-photon coincidence with the Cs $6s^2S$ to $7s^2S$ transition, resulting in a simple practical system with a number of potential applications.

We have since designed and constructed a new Cs IR imaging system that has significantly increased resolution and efficiency. As seen in Table 6.1, this increase was accomplished through higher number density Cs cells of larger area; included for comparison are the parameters of a $LiNbO_3$ up-converter having the same performance. The crystal system requires 1250 times more pump power.

Our most severe technical problem has been the construction of a reliable long-lived Cs cell. The cell used in the demonstration of the IR up-conversion consisted of two metalized sapphire windows brazed to kovar rings. The rings were heliarced to Varian conflat flanges that were then bolted together by means of standard copper gaskets. A nickel side arm was heliarced to the flanges. The cell appeared to fail at the braze between the sapphire and kovar ring.

Because we have encountered difficulties with the construction of the spring-loaded-window Cs cell described in the last status report, we have designed, constructed, and tested another cell. Incorporated in this design are sapphire windows nickel-zirconium brazed to nickel rings. The disadvantage of these windows is that they cannot withstand repeated thermal cycling because of the stress induced by the differing thermal expansion coefficients of nickel and sapphire. Outweighing this disadvantage is the fact that the nickel-zirconium braze is extremely resistant to Cs attack.

Table 6.1

DESIGN PARAMETERS FOR A Cs AND $LiNbO_3$ 2.9 μ UP-CONVERTER

Parameter	Cs	$LiNbO_3$
Pump wavelength (μ)	1.0790	1.06
IR wavelength (μ)	2.94	2.94
Sum wavelength (Å)	4560	7800
Pump bandwidth (cm^{-1})	0.1	$\simeq 1.0$
Pump pulselength (nsec)	50	50
Photon efficiency (%)	27.5	27.5
Resolution	10^5	10^5
Pump power (W)	1.44×10^5	9×10^7
Cs density (cm^{-3})	4.44×10^{17}	---
Area (cm^2)	3.74	2
Length (cm)	0.2	0.46

The new windows were heliarced into Varian conflat flanges and bolted together using copper gaskets, as before. A stainless-steel base was heliarced to the flanges, and this entire assembly was then metal O-ring sealed to the base plate of a vacuum chamber. A side arm was heliarced to the base plate and was also connected to a hole in the base plate by means of a capillary tube. To load the cell, a clean glass ampoule of Cs is inserted in the side arm. Evacuating the outer cell empties the space between the sapphire windows and side arm via the capillary tube. The ampoule is then crushed by flexing the thin-walled side arm. When the side arm is heated, Cs begins to leak out through the capillary tube but condenses at the cold end farthest from the side arm and clogs the tube, thereby sealing off the side arm and cell (Fig. 6.1). Thermal cycling of the window brazes is avoided by keeping the cell body continuously hot although the side arm is allowed to cool between experiments.

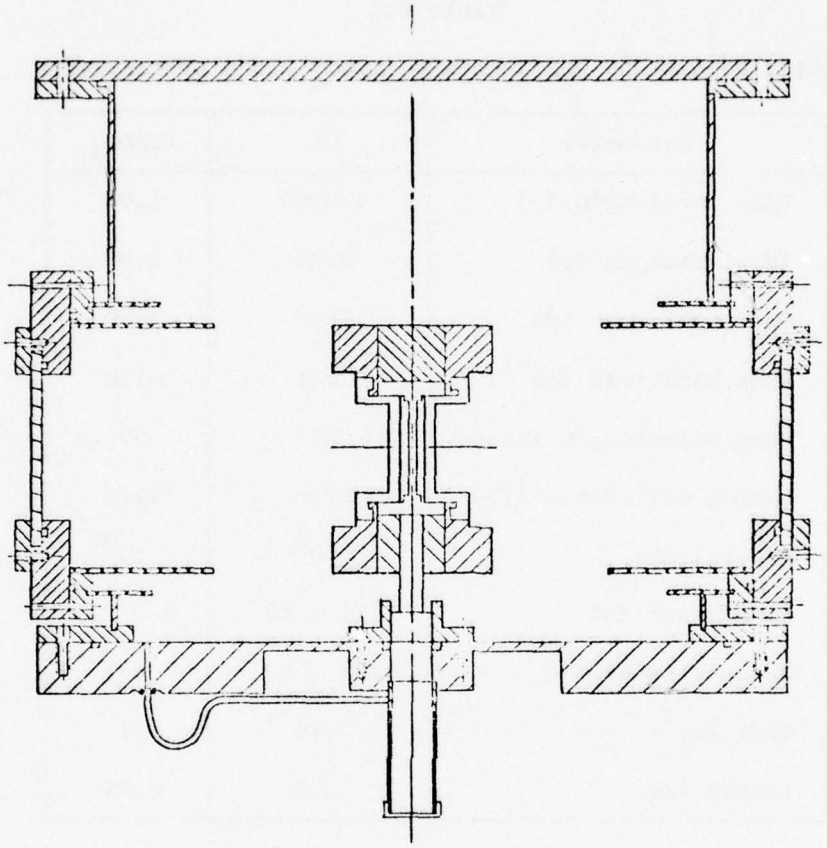

Fig. 6.1. 1--Cs UP-CONVERTER CELL.

This design has proven reliable. The nickel-zirconium brazes have held up well, and there has been no evidence of condensation on the sapphire windows. The vacuum surrounding the cell prevents oxidation of the brazes, copper gaskets, and heater wires.

Using this cell, we have increased the field of view of the up-converter and have measured resolution of the images. Figure 6.2 is a schematic of the experimental setup. With a pump power of 200 kW focused on a 1.1 cm^2 area, a field-of-view of greater than 10,000 resolvable spots has been achieved. This is 10 times greater than our earlier results and approaches TV quality. The Cs cell has an active length of 0.3 cm and can operate at a density of approximately 2×10^{17}/cc. The test object photographed was a metal cut-out resolution test target. The images showed a resolution of at least 12 lines/mm, and the diffraction

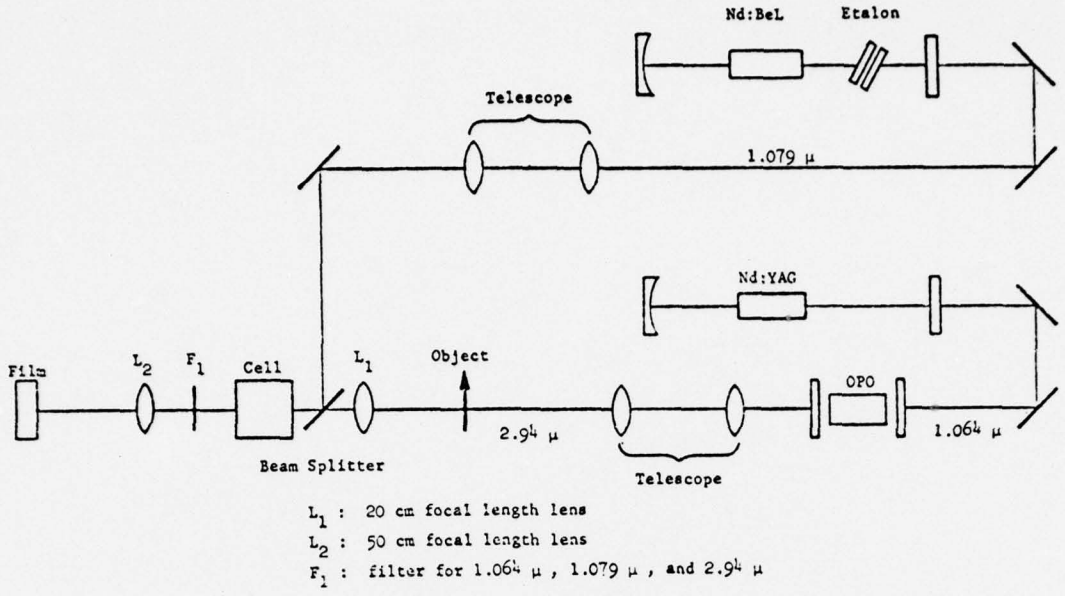

Fig. 6.2. EXPERIMENTAL SETUP.

limit for the optical system was approximately 28 lines/mm. Fine adjustment of the optical components may increase image resolution.

Currently, we are measuring conversion efficiency as a function of Cs density. We will then make still further measurements and characterize image quality.

Appendix A

OUTSIDE PUBLICATIONS

1. Papers Presented at Meetings

Information Systems

Cot, N., "Random Trees with Weighted Branches," Eighth Southeastern Conf. on Combinatorics, Graph Theory, and Computing, Mar 1977.

Cot, N., "Cost of Optimal Prefix Codes," Johns Hopkins Conf. on System Sciences, Apr 1977.

Cover, T., "Multiway Channels and Feedback," Tenth European Meeting of Statisticians, Leuven, Belgium, 22-26 Aug 1977.

Cover, T., "A Rate Region for the Multiple-Access Channel with Feedback," Intl. Conf. on Communications, Chicago, 12-15 Jun 1977.

Cover, T., "The Capacity of Multiple-Access Channels," TRW for ISL Affiliates Program, Los Angeles, 11 May 1977.

Cover, T., "Information Theory and Gambling," IEEE IT Section Meeting, Los Angeles, 11 May 1977.

Friedlander, B., M. Morf, T. Kailath, and L. Ljung, "Levinson- and Chandrasekhar-Type Equations for a General Discrete-Time Linear Estimation Problem," IEEE Decision and Control Conf., Florida, Dec 1976.

Friedlander, B., T. Kailath, and M. Morf, "Embedding the Time-Varying Riccati Equation into Recursive Input-Output Equations," 1977 Conf. on Information Sciences and Systems, Johns Hopkins University, Maryland, 30 Mar-1 Apr 1977.

Friedlander, B., G. Verghese, and T. Kailath, "Scattering Theory and Linear Least-Squares Estimation, Part III: The Estimates," 1977 Conf. on Decision and Control, New Orleans, Dec 1977.

Friedlander, B., T. Kailath, and M. Morf, "A Modified 'Displacement Rank' and Some Applications," 1977 Conf. on Decision and Control, New Orleans, Dec 1977.

Gill, J. and I. Simon, "Polynomial Reducibilities and Upward Diagonalizations," Ninth ACM Symp. on Theory of Computing, Boulder, Colo., May 1977.

Kailath, T., L. Ljung, and M. Morf, "Recursive Input-Output and State-Space Solutions for Continuous-Time Linear Estimation Problems," 1976 IEEE Decision and Control Conf., Florida, Dec 1976.

Kung, S-Y., T. Kailath, and M. Morf, "A Fast Projection Method for Canonical Minimal Realization," 1976 IEEE Decision and Control Conf., Florida, Dec 1976.

Kung, S-Y., T. Kailath, and M. Morf, "Fast and Stable Algorithms for the Minimal Design Problems," IFAC, Canada, 4-8 Jul 1977.

Kung, S-Y., B. Levy, T. Kailath, and G. Verghese, "New Methods for State-Space Realizations," 1977 Conf. on Decision and Control, New Orleans, Dec 1977.

Levy, B., M. Morf, and S-Y. Kung, "New Results in 2-D Systems Theory, Part III: Recursive Realization and Estimation Algorithms for 2-D Systems," Twentieth Midwest Symp. on Circuits and Systems, Lubbock, Texas, Aug 1977.

Levy, B., S-Y. Kung, M. Morf, and T. Kailath, "A Unification of System Equivalence Definitions," 1977 IEEE Conf. on Decision and Control, New Orleans, Dec 1977.

Ljung, L. and T. Kailath, "Formulas for Efficient Change of Initial Conditions in Linear Least-Squares Estimation," 1976 IEEE Decision and Control Conf., Florida, 1976.

Morf, M., E. Verriest, J. Dobbins, and T. Kailath, "Square-Root Algorithms for Model Sensitivity Analysis," 1977 Conf. on Information Sciences and Systems, Johns Hopkins University, Maryland, 30 Mar-1 Apr 1977.

Morf, M., A. Vieira, D. T. Lee, and T. Kailath, "Recursive Multichannel Maximum Entropy Method," 1977 JACC, San Francisco, Jun 1977.

Morf, M., B. Levy, and T. Kailath, "Square-Root Algorithms for the Continuous-Time Linear Least-Squares Estimation Problem," 1977 IEEE Conf. on Decision and Control, New Orleans, Dec 1977.

Verghese, G. and T. Kailath, "Fixing the State-Feedback Gain by Choice of Closed-Loop Eigensystem," 1977 IEEE Conf. on Decision and Control, New Orleans, Dec 1977.

Digital Systems

Lee, R. B-L., "Performance Bounds in Parallel Processor Organizations," Symp. on High-Speed Computers and Algorithm Organization, University of Illinois, Champaign, 13-15 Apr 1977.

Integrated Circuits

Estreich, D. B. and R. W. Dutton, "Modeling Integrated Injection Logic (I^2L) Performance and Operational Limits," Intl. Solid-State Circuits Conf., Philadelphia, 16 Feb 1977.

Estreich, D. B. and R. W. Dutton, "A User-Oriented I^2L Macromodel," WESCON, San Francisco, 20 Sep 1977; included in "Designing with Integrated Injection Logic: I^2L Comes of Age," session 11, WESCON/1977.

Solid State

Garner, C. M., Y. D. Shen, G. L. Pearson, and W. E. Spicer, "Auger Profiling of $Al_xGa_{1-x}As$-Ga-As Heterojunctions Grown by LPE," Am. Phys. Soc., San Diego, California, 21 Mar 1977.

Radioscience

Bhatnager, N., M. S Frankel, and A. M. Peterson, "Interaction of Electromagnetic and Acoustic Waves in a Stochastic Atmosphere," URSI Commission F Open Symp. on Propagation in Nonionized Media, La Bule, France, 28 Apr-6 May 1977.

Frankel, M. S, N. Bhatnager, and A. M. Peterson, "Interaction of Electromagnetic and Acoustic Waves in a Quiescent Atmosphere To Measure Temperature and Horizontal Winds," URSI/USNC Symp., Stanford University, 22-24 Jun 1977.

2. Papers Published

Information Systems

Cover, T. and J. van Campenhout, "On the Possible Orderings in the Measurement-Selection Problem," IEEE Trans. on Systems, Man, and Cybernetics, SMC-7, Sep 1977, pp. 657-661.

Cover, T. and A. Shenhar, "Compound Bayes Predictors for Sequences with Apparent Markov Structure," IEEE Trans. on Systems, Man, and Cybernetics, SMC-7, Jun 1977, pp. 421-424.

Cover, T., "Comments on Stone's Paper," Ann. of Stat., 5, Jul 1977, pp. 627-628.

Gray, R., "Time-Invariant Trellis Encoding of Ergodic Discrete-Time Sources with a Fidelity Criterion," IEEE Trans. on Information Theory, 23, Jan 1977, pp. 71-83.

Gray, R. and A. H. Gray, Jr., "Asymptotically Optimal Quantizers," IEEE Trans. on Information Theory, 23, Feb 1977, pp. 143-144.

Gray, R., A. H. Gray, Jr., and J. D. Markel, "Comparison of Optimal Quantizations of Speech-Reflection Coefficients," IEEE Trans. on Acoustics, Speech, and Signal Processing, 25, Feb 1977.

Gray, R. and P. C. Shields, "The Maximum Mutual Information between Two Random Processes," Information and Control, 33, Apr 1977, pp. 273-280.

Kailath, T. and L. Ljung, "A Scattering Theory Framework for Fast Least-Squares Algorithms," in Multivariate Analysis--IV, North-Holland Publishing Co., 1977, pp. 387-406.

Kailath, T., L. Ljung, and M. Morf, "Generalized Krein-Levinson Equations for Efficient Calculation of Fredholm Resolvents of Nondisplacement Kernels," Advances in Mathematics, 1977.

Kailath, T. (ed.), Linear Least-Squares Estimation, Benchmark Papers in Electrical Engineering and Computer Sciences, Dowden, Hutchinson, & Ross, Inc., Stroudsburg, Pennsylvania, 1977.

Kung, S-Y., B. Levy, M. Morf, and T. Kailath, "New Results in 2-D Systems Theory, Part II: 2-D State-Space Models--Realization and the Notions of Controllability, Observability, and Minimality," Proc. IEEE, 65, Jun 1977, pp. 945-961.

Ljung, L. and T. Kailath, "Efficient Change of Initial Conditions, Dual Chandrasekhar Equations, and Some Applications," IEEE Trans. on Automatic Control, AC-22, Jun 1977, pp. 443-447.

Morf, M. and T. Kailath, "Recent Results in Least-Squares Estimation Theory," Ann. of Economic and Social Measurement, 6, 1977, pp. 261-274.

Morf, M., B. Levy, and S-Y. Kung, "New Results on 2-D Systems Theory, Part I: 2-D Polynomial Matrices, Factorization, and Coprimeness," Proc. IEEE, 65, Jun 1977, pp. 861-872.

Rosenfeld, D. and A. Macovski, "Time-Modulated Apertures for Tomography in Nuclear Medicine," IEEE Trans. on Nuclear Science, NS-24, Feb 1977.

Vieira, A. and T. Kailath, "On Another Approach to the Schur-Cohn Criterion," IEEE Trans. on Circuits and Systems, 25, Apr 1977, pp. 218-220.

Widrow, B. and J. M. McCool, "A Comparison of Adaptive Algorithms Based on the Methods of Steepest Descent and Random Search," IEEE Trans. on Antennas and Propagation, AP-24, Sep 1976, pp. 615-637.

Widrow, B. et al, "Stationary and Nonstationary Learning Characteristics of the LMS Adaptive Filter," Proc. IEEE, 64, Aug 1976, pp. 1151-1162.

Widrow, B. et al, "Reply to D. F. Tufts on Adaptive Spectral Estimation," Proc. IEEE, Jan 1977, pp. 171-173.

Digital Systems

Iliffe, J. K., "Interpretive Machines," TR No. 149, Digital Systems Laboratory, Stanford University, Stanford, Calif., Jun 1977.

Iliffe, J. K., "Computing in Store," Tech. Note No. 117, Digital Systems Laboratory, Stanford University, Stanford, Calif., Jun 1977.

Owicki, S. S., "Verifying Concurrent Programs with Shared Data Classes," TR No. 147, Digital Systems Laboratory, Stanford University, Stanford, Calif., 1977.

Rossetti, D. J. and T. H. Bredt, "The Design and Implementation of an Operating System Tracer," Tech. Note No. 97, Digital Systems Laboratory, Stanford University, Stanford, Calif., 1977.

vanCleemput, W. M., "Hypergraph Models for the Circuit Layout Problem," Appl. Math. Modeling, 1, Dec 1976, pp. 160-161.

vanCleemput, W. M., "A Structural Design Language for Computer-Aided Design of Digital Systems," TR No. 130, Digital Systems Laboratory, Stanford University, Stanford, Calif., Apr 1977.

vanCleemput, W. M., "An Algorithm for Testing the Planarity of Partially Oriented Graphs," Tech. Note No. 116, Digital Systems Laboratory, Stanford University, Stanford, Calif., Jun 1977.

vanCleemput, W. M., "On the Planarity of Hypergraphs," TR No. 115, Digital Systems Laboratory, Stanford University, Stanford, Calif., Jun 1977.

vanCleemput, W. M., T. C. Bennett, J. A. Hupp, and K. R. Stevens, "SPRINT--An Interactive System for Printed Circuit Board Design User's Guide," TR No. 143, Digital Systems Laboratory, Stanford University, Stanford, Calif., Jun 1977.

Integrated Circuits

Estreich, D. B., R. W. Dutton, and B. W. Wong, "An Integrated Injection Logic (I^2L) Macromodel Including Current Redistribution Effects," IEEE J. Solid-State Circuits, SC-11, Oct 1976, pp. 648-657.

Solid State

Cheng, K. Y. and G. L. Pearson, "The Al-Ga-Sb Ternary Phase Diagram and Its Application to Liquid Phase Epitaxy Growth," J. Electrochem. Soc., 124, May 1977, pp. 753-757.

Garner, C. M., Y. D. Shen, J. S. Kim, G. L. Pearson, W. E. Spicer, J. S. Harris, and D. D. Edwall, "Auger Profiling of 'Abrupt' LPE $Al_xGa_{1-x}As$-GaAs Heterojunctions," J. Appl. Phys., 48, Jul 1977, pp. 3147-3149.

Garner, C. M., Y. D. Shen, J. S. Kim, G. L. Pearson, W. E. Spicer, J. S. Harris, D. D. Edwall, and R. Sahai, "Auger Depth Profiling of Au-Al_xGa_{1-x} As Interfaces and LPE $Al_xGa_{1-x}As$-GaAs Heterojunctions," J. Vac. Sci. Tech., 14, Jul/Aug 1977, pp. 985-988.

Radioscience

Bhatnager, N., "Interaction of Electromagnetic and Acoustic Waves in a Stochastic Atmosphere," Ph.D. dissertation, Stanford Electronics Laboratories, Stanford University, Stanford, Calif., Jul 1977.

Frankel, M. S, N. J. F. Chang, and M. J. Sandero, "A High Frequency Radio Acoustic Sounder for Remote Measurement of Atmospheric Winds and Temperature," Bull. Amer. Meteorol. Soc., Sep 1977.

Wernecke, S. J. and L. R. D'Addario, "Maximum Entropy Image Reconstruction," IEEE Trans. on Computers, C-26, Apr 1977, p. 351.

3. Papers Accepted for Publication

Information Systems

Cover, T. and C. Keilers, "An Offensive Statistic for Baseball," JORSA.

Cover, T. and R. King, "A Convergent Gambling Estimate of the Entropy of English," IEEE Trans. on Information Theory.

Cover, T. and S. K. Leung-Yan-Cheong, "Some Inequalities between Shannon Entropy and Kolmogorov, Chaitin, and Extensions Complexities," IEEE Trans. on Information Theory.

Friedlander, B., M. Morf, T. Kailath, and L. Ljung, "New Inversion Formulas for Matrices Classified in Terms of Their Distance from Toeplitz Matrices," SIAM J. on Applied Mathematics.

Friedlander, B., T. Kailath, and M. Morf, "A Modified Displacement Rank and Some Applications," IEEE Trans. on Automatic Control.

Gill, J., "Computational Complexity of Probabilistic Turing Machines," SIAM J. on Computing.

Gill, J. and G. Miller, "Newton's Method and Ratios of Fibonacci Numbers," Fibonacci Quarterly.

Gray, R., "Second-Order Moments and Prediction for Doubly Reflected Symmetric Independent Increment Processes," SIAM J. Appl. Math.

Gray, R. and M. B. Pursley, "Source Coding Theorems for Stationary, Measurable, Continuous-Time Stochastic Processes," Ann. Prob.

Kailath, T., L. Ljung, and M. Morf, "Generalized Krein-Levinson Equations for Efficient Calculation of Fredholm Resolvents of Nondisplacement Kernels," Advances in Mathematics.

Kailath, T., L. Ljung, and M. Morf, "Recursive Input-Output State-Space Solutions for Continuous-Time Linear Estimation Problems," IEEE Trans. on Automatic Control.

Kailath, T., A. Vieira, and M. Morf, "Inverses of Toeplitz Operators, Innovations, and Orthogonal Polynomials," SIAM Rev.

Kung, S-Y., B. Levy, T. Kailath, and G. Verghese, "New Methods for State-Space Realizations," IEEE Trans. on Automatic Control.

Leung-Yan-Cheong, S. K. and M. E. Hellman, "The Gaussian Wiretap Channel," IEEE Trans. on Information Theory.

Levy, B., M. Morf, and S-Y. Kung, "New Results in 2-D Systems Theory, Part III: Recursive Realization and Estimation Algorithms for 2-D Systems," IEEE Trans. on Acoustics, Speech, and Signal Processing.

Morf, M., B. Dickinson, T. Kailath, and A. Vieira, "Efficient Solution of Covariance Equations for Linear Prediction," IEEE Trans. on Acoustics, Speech, and Signal Processing.

Morf, M., T. Kailath, and B. Dickinson, "A Class of Fast Least-Squares Algorithms," IEEE Trans. on Acoustics, Speech, and Signal Processing.

Morf, M., B. Levy, and T. Kailath, "Square-Root Algorithms for the Continuous-Time Linear Least-Squares Estimation Problem," IEEE Trans. on Automatic Control.

Vieira, A. and T. Kailath, "On Another Approach to the Schur-Cohn Criterion," IEEE Trans. on Circuits and Systems.

Widrow, B. and J. M. McCool, "Comments on 'An Adaptive Recursive LMS Filter'," Proc. IEEE.

Digital Systems

Lee, R. B-L., "Performance Bounds in Parallel Processor Organizations," Proc. of Symp. on High-Speed Computers and Algorithm Organization, Academic Press, New York, in press.

vanCleemput, W. M., "A Hierarchical Language for the Structural Description of Digital Systems," Proc. of Fourteenth Design Automation Conf., New Orleans, in press.

vanCleemput, W. M., "On the Planarity of Hypergraphs," Proc. IEEE.

Integrated Circuits

Estreich, D. B. and R. W. Dutton, "Modeling Integrated Injection Logic (I^2L) Performance and Operational Limits," IEEE J. Solid-State Circuits, SC-12, Oct 1977.

Solid State

Kocot, K. and G. L. Pearson, "Experimental Verification of Cr^{2+} Models of Photoluminescent Transitions in GaAs:Cr and $Al_xGa_{1-x}As$:Cr Single Crystals," Solid State Communications.

Miller, J., I. Lindau, and W. E. Spicer, "The Electronic Structure of Clean and Oxidized Niobium," Intl. Conf. on Physics of Transition Metals, in press.

Radioscience

Leuenberger, K., R. W. Lee, and A. T. Waterman, "Remote Atmospheric Probing on a Line-of-Sight Path, Using Spatial Filter Concepts. I: Theory," Radio Science.

Wernecke, S. J., "Two-Dimensional Maximum Entropy Reconstruction of Radio Brightness," Radio Science.

Appendix B

ABSTRACTS OF REPORTS PUBLISHED DURING THIS PERIOD

This appendix is a compilation of abstracts of reports issued by the Stanford Electronics Laboratories (SEL).

PREPARATION AND PROPERTIES OF
SEMI-INSULATING LIQUID PHASE
EPITAXIAL GALLIUM ARSENIDE
FOR APPLICATION TO FET DEVICES
by Yu-Min Houng

ARPA through Rockwell ISC
Contract F19628-75-C-0113
Subcontract 52377
TR No. 5125-1
January 1977

ABSTRACT

The growth of high resistance liquid-phase epitaxial (LPE) GaAs layers requires close-compensation of shallow donors and acceptors arising from residual impurities in the source materials and from chemical reactions between the growth system components. Once near-compensation is attained, further improvements can be obtained by the addition of chromium (Cr), which forms deep acceptor levels, thus yielding semi-insulating LPE GaAs. High resistance LPE layers having sheet resistances of 10^5 ohms/□ or more and low deep level impurity concentrations can be used as buffer layers in GaAs field effect transistors (FET) to improve device performance.

Three different horizontal tilt LPE growth systems were investigated. These in order of investigation were SiO_2-C-H_2, SiO_2-BN(C)-H_2, and SiO_2-BN-H_2 systems. It was found that the chemical reactions in each of these systems can be controlled by systematic bakeouts of the arsenic-saturated gallium melts before each growth. Low bakeout temperatures provided *n*-type layers while high bakeout temperatures gave p-type layers and a critical intermediate bakeout temperature, unique to each system, gave high resistivity layers with N_A/N_D close to 1. The transition bakeout temperatures for the SiO_2-C-H_2, SiO_2-BN(C)-H_2, and SiO_2-BN-H_2 systems were found to be 775, 700, and 675°C, respectively. The dominant impurities were found to be silicon, carbon, and oxygen. Their relative concentrations were functions of bakeout temperature and were responsible for the conductivity type transition of the grown layers.

The optimum growth conditions for growing high resistance LPE layers in each of these systems were established. The optimum compensated layers grown in these systems without deep level impurity doping had resistivities as high as 700 ohm-cm and sheet resistances in the range of 5×10^5 ohms/□. Semi-insulating layers with resistivities up to 5×10^6 ohm-cm and sheet resistances above 10^9 ohms/□ were grown in the SiO_2-BN(C)-H_2 system from Ga melts doped with 0.5 atm.% Cr and baked out at the transition temperature.

The transport related properties of semi-insulating LPE GaAs were investigated. Photoluminescence measurements showed a dominant peak at 0.83 eV in both Cr-doped GaAs commercial substrates and grown LPE layers. The temperature variation of conductivity and the Hall coefficient of Cr-doped semi-insulating LPE layers were studied using differential van der Pauw techniques. The thermal activation energies of these layers were in the range of 0.7 eV. The compensation ratios in these layers were found to be in the range of 1.4-2.6, and the deep level concentrations were estimated to be in the low 10^{14} cm^{-3} range.

Transient capacitance measurements were made to study the interface properties of FET type devices with and without LPE buffer layers. No detectable traps were found in the buffered devices whereas two deep hole traps, located 0.58 and 0.81 eV above the valence band, were detected in the unbuffered FET devices when the gate depletion region approached the substrate interface. The trap concentrations were 1×10^{16} and 2×10^{15} cm^{-3}, respectively. An interface model was developed and used to successfully explain that the minority carrier trapping effects which appeared in the active layer were due to the image effect of majority carrier traps in the Cr-doped substrate acting through the interface space-charge region. The results of this work are a positive demonstration of the usefulness of buffer layers in FET devices prepared on semi-insulating GaAs substrates.

PERFORMANCE BOUNDS FOR
PARALLEL PROCESSORS
by Ruby Bei-Loh Lee

JSEP Contract
N00014-75-C-0601
TR No. 125
November 1976

ABSTRACT

A general model of computation on a p-parallel processor is proposed, distinguishing clearly between the logical parallelism (p* processes) inherent in a computation and the physical parallelism (p processors) available in the computer organization. This shows the dependence of performance bounds on both the computation being executed and the computer architecture. We formally derive necessary and sufficient conditions for the maximum attainable speedup of a p-parallel processor over a uniprocessor to be $Sp \leq \min(\frac{p}{\ln p}, \frac{p^*}{\ln p^*})$, where $\ln p$ approximates H_p, the p^{th} harmonic number. We also verify that empirically-derived speedups are $O(\frac{p^*}{\ln p^*})$. Finally, we discuss related performance measures of minimum execution time, maximum efficiency, and minimum space-time product.

SPREADING RESISTANCE
FOR IMPURITY PROFILES
by Donald C. D'Avanzo,
Robert D. Rung, and
Robert W. Dutton

Industrial Grant from
H-P Co. Corp. Eng. and
NSF Contract ENG-74-12151
TR No. 5013-2
February 1977

ABSTRACT

The objective of this report is to describe the spreading resistance method for determination of impurity profiles, as implemented in the Stanford University Integrated Circuit Laboratory. The main topics that are considered include the measurement technique, analysis of the data, accuracy limitations and applications.

Discussion of sample preparation focuses on the relative bevel quality achieved with various polishing compounds. A technique for accurately measuring bevel angles on the order of 16' is outlined. The non-ideal nature of the spreading resistance to resistivity calibration is discussed with respect to probe contact characteristics, sample preparation and orientation and impurity type. The multilayer correction method and an efficient implementation algorithm are presented.

Comparison of spreading resistance with incremental sheet resistance measurements reveals both the overall usefulness and accuracy as well as the limitations of the technique. Several causes for the discrepancies in the comparison are proposed and future areas of investigation are suggested. Finally, several applications are presented, including process development and characterization, device modeling and process simulation.

HIGH VOLTAGE CMOS
INTEGRATED CIRCUITS
by Gerald Alan May

Industrial Gifts from Xerox
and NSF Grant ENG75-22329
Tech. Summary Rep. No. 4834-2
January 1977

ABSTRACT

A new high voltage silicon-gate simultaneous diffusion CMOS process has been introduced in this study. Low voltage (15 V) high-density silicon-gate CMOS is fabricated on the same integrated circuit die as high voltage (160 V) p-channel transistors. This feature permits for the first time the design of high voltage, low power integrated circuits needed in biomedical applications with the low voltage signal processing circuitry and high voltage drive circuitry on the same monolithic substrate.

Several types of high voltage p-channel transistors were developed. By incorporating a lightly doped, deep p^- diffusion for the drain region, a high voltage device with a thin gate oxide for high transconductance has been fabricated to operate with -160 volts at the drain-substrate junction. In addition, by utilizing a previously reported field plate principle, a polycrystalline field plate surrounding the p^- drain junction increases the breakdown of the high voltage p-channel transistor to -300 volts. The breakdown characteristics of these transistors have been explained by a two dimensional computer aided solution to Poisson's equation. The field crowding occurring under the gate oxide in conventional MOS transistors with shallow p^+ drain diffusions is shown to be reduced in the deep p^- diffusion. Both of the high voltage transistors can be easily fabricated using conventional silicon-gate processing technology.

The high voltage CMOS technology provides the first such process to make possible the realization of all of the low power custom circuitry necessary for the development of a compact, light weight, one-hand reading aid for the blind (Optacon). A high voltage micropower CMOS tactile display driver multiplexer has been developed to drive the piezoelectric transducers in the tactile screen of the custom CMOS Optacon system. A novel push-pull bootstrapping output driver is employed to gate 100 volt square waves to high capacitive loads (such as piezoelectric transducers). Using positive feedback from source to gate of the high voltage device enables the push-pull output stage to be driven from low voltage CMOS

circuitry. Each output stage can deliver 9 milliwatts to the load while consuming less than 500 microwatts.

A new trichloroethylene (TCE) oxidation technology is incorporated into the CMOS fabrication process. The TCE oxidation results in greater oxide stability and longer MOS capacitor storage times. The average dielectric breakdown strength is also improved and the frequency of low field oxide breakdown is reduced. The TCE oxidation improves the high voltage device properties by exhibiting faster junction breakdown walkout with lower hot electron injection current into the gate oxide.

SUPREM I--A PROGRAM FOR
IC PROCESS MODELING AND
SIMULATION

by Dimitri A. Antoniadis,
Stephen E. Hansen,
Robert W. Dutton, and
Adalberto G. Gonzales

Army Research Office
Contract DAAG-29-77-C-006
TR No. 5019-1
May 1977

ABSTRACT

The first version of the Stanford University IC process simulator program, SUPREM, is described. The first part of this report outlines the development of numerical models for the one-dimensional redistribution of impurities in silicon resulting from moving boundaries as in oxidation and epitaxy. Also described is the diffusion model used in SUPREM to simulate concentration dependent diffusivities and cooperative diffusion. The second part (Appendix 1) contains the operation manual for SUPREM which describes in detail the user-program interfacing. The last part of the report (Appendix 2) consists of an example of program usage to simulate a multi-step process together with the resulting outputs.

SUPPRESSION EFFECTS
ASSOCIATED WITH VLF
TRANSMITTER SIGNALS
INJECTED INTO THE
MAGNETOSPHERE
by Rajagopalan Raghuram

Office of Naval Research
Contract Nonr N00014-76-0689
NSF Atmospheric Sciences Sec.
Grant ATM75-07707 A1,2
NSF Div. of Polar Programs
Grant DPP-74-0493 A1,2
TR No. 3456-3
March 1977

ABSTRACT

Magnetospheric growth of coherent VLF signals transmitted from Siple Station, Antarctica is inhibited by whistler mode echoes of earlier transmitter signals. This new phenomenon, called echo-induced suppression, is observed at least a third of the time that transmissions from Siple Station are detected at the receiving station in Roberval, Quebec, Canada. Suppression levels as high as 20 dB are observed. Though the echo is usually much weaker than the direct signal, the level of suppression is directly related to the amplitude of the echo. The echoes reduce triggering of emissions as well as the growth of the signal. Echo-induced suppression is not explained by linear wave-wave interference. The echoes are thought to restrict growth by reducing the coherence of the total input signal. According to quasi-linear theory, wave growth is regulated by changes in the particle pitch angle distribution that results from wave-particle interaction. These new results suggest that coherent waves tend to limit their own growth, even when modification of the particle pitch angle distribution is unimportant. Other phenomena such as whistler-induced suppression of signal growth are thought to be related to echo-induced suppression. Wave-induced growth suppression provides an indirect verification of the existence of discrete ducts for the propagation of VLF signals in the magnetosphere. Another suppression phenomenon, also discovered from VLF transmissions, is the suppression of mid-latitude hiss by as much as 6 dB in a band up to 200 Hz wide just below the transmitter frequency. This quiet band develops in 5 to 25 s and lasts up to a minute after the end of transmissions. There is evidence that power-line radiation in the magnetosphere at harmonics of 60 Hz also produces quiet bands. Quiet bands are explained by pitch angle scattering of electrons before they reach the growth region near the equator. A change in the distribution function of electrons in the appropriate parallel velocity range is thought to be responsible for the quiet band. Quiet bands lead to indirect estimates of duct widths, scattering regions and perturbations in electron distribution functions.

SEQUENTIAL PREFETCH
STRATEGIES FOR IN-
STRUCTIONS AND DATA
by B. Ramakrishna Rau

ERDA Contract
EY-76-S-03-0326-PA 39
Computer time at SLAC
TR No. 131
SU-326-P.39-18
January 1977

ABSTRACT

An investigation of sequential prefetch as a means of reducing the average access time is conducted. The use of a target instruction buffer is shown to enhance the performance of instruction prefetch. The concept of generalized sequentiality is developed to enable the study of sequentiality in data streams. Generalized sequentiality is shown to be present to a significant degree in data streams from measurements on representative programs. This result is utilized to develop a data prefetch mechanism which is found to be capable of anticipating, on the average, about 75% of all data requests.

A NEW MODEL FOR BORON
DIFFUSION IN SILICON
by John Ross Anderson

NSF Grant GH-31999
TR No. 4737-1
May 1976

ABSTRACT

A new model for boron diffusion in silicon is proposed in which the dominant diffusing species is a neutral boron-vacancy pair. These pairs, each consisting of a negatively charged boron atom and a positively charged vacancy, repeatedly form and breakup, establishing a boron distribution in the silicon. The boron profile is determined by the simultaneous solution of the diffusion equations for boron and boron-vacancy pairs, where the diffusion coefficient of boron by itself is assumed to be negligible. However, since boron does get into the lattice by the diffusion and breakup of boron-vacancy pairs, an apparent boron diffusion coefficient can be determined and is found to be equal to the ratio of boron-vacancy pair concentration to unpaired boron concentration times, the boron-vacancy diffusivity. It is this apparent boron diffusion coefficient that appears in the literature.

The model also explains the concentration dependence of the apparent boron diffusion coefficient, although the boron-vacancy diffusion coefficient is not concentration dependent.

However, the lifetime and diffusion coefficient of boron-vacancy pairs are not readily determinable from thermal diffusion data.

The boron-vacancy diffusion model is also shown to fit data from proton-enhanced diffusion of boron in silicon. In particular, it successfully explains the dip in the electrically active boron concentration often seen near the proton projected range after a proton bombardment. In addition, the boron-vacancy diffusion coefficient and lifetime may be estimated from proton-enhanced diffusion experiments. At 750°C the boron-vacancy diffusion coefficient is estimated to be 5.7×10^{-14} cm^2/sec and lifetime is estimated to be 4.5×10^3 sec. The value found for the boron-vacancy diffusion coefficient is about 4000 times the expected value for the apparent intrinsic diffusion coefficient of boron at 750°C.

Qualitative arguments are presented to show that a similar impurity-vacancy diffusion model is likely for donor dopants in silicon. Also qualitative arguments are presented showing that two such species diffusion effects as emitter dip, emitter push, and emitter pull can be described by impurity-vacancy diffusion models.

A THEORETICAL APPROACH TO THE CALCULATIONS OF ANNEALED IMPURITY PROFILES OF ION IMPLANTED BORON INTO SILICON

by Alejandro Chu

DARPA Contract
DAA-B07-75-C-1344
NSF Grant GH-31999
TR No. 4969-2
May 1977

ABSTRACT

A multi-stream diffusion model is proposed for the calculation of the annealing behavior of boron that is ion implanted into silicon at room temperature and subsequently annealed. This model is capable of predicting both the redistribution and the electrical activation of boron during the anneal, as a realistic model should. The calculated results compare very well with extensive experimental data reported in the literature. The comparison includes samples that are implanted at room temperature with boron in the dose range from 10^{14} to 10^{16} ions/cm^2 and subsequently annealed in the temperature range from 800°C to 1000°C. This range of dose and annealing conditions includes both the typical applications of ion implantation as it is applied in the fabrication of devices and the unconventional cases of high dose implants and low temperature annealing.

The annealing model is in essence a diffusion model extended to include the following situations:

(1) precipitation of boron, when the boron concentration level exceeds the solid solubility limit, in high dose implantation cases

(2) trapping of boron by the strain fields associated with dislocation dipoles that form during annealing at low temperature

In both cases, the presence of this immobile and electrically inactive boron alters significantly the redistribution and electrical activation behavior of boron during the anneal.

The presence of boron precipitates makes it necessary to include four species in the annealing model. These species are substitutional (electrically active) boron, boron-vacancy pairs (electrically inactive), positively charged vacancies, and the aforementioned immobile boron. The electrically active boron is assumed to diffuse substitutionally by means of random encounters with neutral vacancies. The boron-vacancy pair is

assumed to diffuse much more rapidly. The principal interaction among the species is the reaction of active boron with positive vacancies to form BV-pairs.

The parameters in the model are a set of diffusivities and lifetimes for various species and interaction. These parameters are estimated from the examination of each diffusion and each interaction. The values of the most important parameters obey simple activation energy relations. In other cases, the modelling was either not carried to the extent necessary as to make the temperature dependence apparent, or else the parameters represent the composite effects of very complex interactions. In all cases, the mathematical model and the parameter set are universal in the sense that the same equations and parameters can be used for the prediction of ordinary diffusion, proton enhanced diffusion, and the annealing behavior of ion implanted boron at room temperature under conditions that include precipitation effects and low annealing temperature anomalies. Furthermore, in most cases of practical importance, high dose and low annealing temperature conditions are of limited interest and, as a result, the three stream diffusion model with an appropriate subset of parameters is sufficient. This reduced model is still very important and attractive because, once the parameters associated with high dose and/or low temperature anomalies are deleted, the remaining parameters have simple activation energies and are determined by the specification of a single variable: the temperature.

AIR/UNDERSEA COMMUNICATION
AT ULTRA-LOW-FREQUENCIES
USING AIRBORNE LOOP ANTENNAS
by A. C. Fraser-Smith, D. M.
Bubenik, and O. G. Villard, Jr.

DARPA (ARPA Order No.
1733) through the ONR
Contract N00014-75-C-1095
TR No. 4207-6
June 1977

ABSTRACT

In this report we investigate the possibility of using ultra-low-frequency (ULF) signals from airborne loop antennas (i.e., magnetic dipoles) for air/undersea communication. Because of the low data rate at ULF, communication is here understood to mean the transfer of short messages of high information content.

We use numerical integration to calculate the 1 Hz total magnetic field amplitudes in the sea at depths from 0 m to 200 m due to airborne unit moment vertical and horizontal magnetic dipoles at altitudes from 100 m to 10 km. Considering the magnetic moments m attainable with present aircraft power and payload capability ($m = 10^7$ A m^2 - 10^9 A m^2) and the minimum detectable amplitude for a 1 Hz signal beneath the sea (~1 mγ), we conclude that air/undersea communication at 1 Hz is possible under the following illustrative conditions: For a horizontal plane loop antenna at 3000 m altitude and a ULF receiver at a 100 m depth, communication is possible for horizontal distances to 10 km for $m = 10^7$ A m^2 and to 33 km for $m = 10^9$ A m^2. The corresponding limits for a vertical plane loop antenna are 13 km to 64 km. It is also possible, if desired, to limit communication to a comparatively small circular area directly beneath the aircraft. Sea floor effects can alter these values significantly, particularly if the receiver is near the floor.

A STRUCTURAL DESIGN LANGUAGE FOR COMPUTER AIDED DESIGN OF DIGITAL SYSTEMS

by W. M. vanCleemput

JSEP Program Contract
N00014-75-C-0601
TR No. 136
April 1977

ABSTRACT

In this report a language (SDL) for describing structural properties of digital systems will be presented. SDL can be used at all levels of the design process, i.e., from the system level down to the circuit level. The language is intended as a complement to existing computer hardware description languages which emphasize behavioral description. The language was motivated partly by the nature of the design process.

TOTALLY IMPLANTABLE BIDIRECTIONAL PULSED DOPPLER BLOOD FLOW TELEMETRY: INTEGRATED TIMER-EXCITER CIRCUITRY AND DOPPLER FREQUENCY ESTIMATION

by Henry V. Allen

PHS Research Grant
P01 GM17940
Department of Health, Education and Welfare
TR No. 4958-4
May 1977

ABSTRACT

Although blood flow is one of the basic parameters desired in physiological studies, it has proven to be elusive to obtain because of baseline and scale-factor drift in currently available flowmeters. A new totally implantable bidirectional pulsed doppler blood flowmeter resolves these problems. Based on two custom-designed integrated circuits (ICs), this device measures $2.9 \times 3.8 \times 0.8$ cm^3 and is the smallest implantable flowmeter realized to date. This report describes the design of portions of the system intended for long-term implantation in chronic animal research.

The effects of noise sources in the timing portion of the flowmeter are analyzed through a simple first-order approach; this jitter produces spectral broadening of doppler returns and excessive noise near such strong reflections as vessel walls. Equations are developed to quantify these effects.

Quadrature direction-sensing techniques are compared with offset techniques. Infinite attenuation of low-frequency artifacts in the doppler returns is the primary reason for pursuing the quadrature approach; another major factor is that it adds minimally to the implantable-system complexity and power requirements.

The timer-exciter IC sets the ultrasonic frequency, repetition rate of the ultrasonic burst, and the burst length. This IC contains over 80 transistors, 75 resistors, and 300 pF of capacitance for six integrated MOS capacitors. The circuit has a power drain of 3.6 mA at 2.75 V for a 20 kHz repetition rate and a 1.5 μsec output burst. Timing jitter is limited to the extent that noise caused by strong reflections increases by only 4 dB over the normal receiver noise, and spectral broadening is less than 50 Hz. A novel triple one-shot chain is introduced that requires only a single timing capacitor. Rapid resynchronization of the ultrasonic oscillator provides coherence between it and the repetition rate, and the capability to operate either in the pulsed or continuous-wave mode allows this IC to be used in both these types of doppler ultrasonic flowmeters.

A further innovation is a frequency estimator that employs zero-crossing information to determine the magnitude and sign of the doppler flow signal; unlike other zero-crossing counters, however, this system measures the center frequency of wideband gaussian noise which is statistically similar to doppler returns. This estimator uses four zero crossings and is the first such processor specifically designed, tested, and intended for doppler flow measurements.

Contributions in four areas--timer stability, direction sensing, integrated-circuit design and development, and frequency estimation--provide a necessary basis for producing a miniature pulsed doppler flowmeter. However, these areas represent only part of the total effort that has been required to accomplish this task. The works of R. W. Gill and J. W. Knutti of Stanford University are also instrumental in the successful implementation of this system.

ON ACCURACY IMPROVEMENT AND APPLICABILITY CONDITIONS OF DIFFUSION APPROXIMATION WITH APPLICATIONS TO MODELLING OF COMPUTER SYSTEMS

by Philip S. Yu

Ballistic Missile Defense
Systems Command Contract
DASG60-77-C-0073
Computer time at SLAC
TR No. 129
January 1977

ABSTRACT

Starting with single server queueing systems, we find a different way to estimate the diffusion parameters. The boundary condition is handled using the Feller's elementary return process. Extensive comparisons by asymptotic, simulation and numerical techniques have been conducted to establish the superiority of the proposed method compared with conventional methods. The limitation of the diffusion approximation is also investigated. When the coefficient of variation of interarrival time is larger than one, the mean queue length may vary over a wide range even if the mean and variance of interarrival time are kept unchanged. The diffusion approximation is applicable under the condition that the high variation of interarrival time is due to a large number of short interarrival times. Case studies are conducted on 2-stage hyperexponential distributions. A similar anomaly is observed in two server closed queueing networks when the service time of any server has a large coefficient of variation. Again, a similar regularity condition on the service time distribution is required in order for the diffusion approximation to be applicable. For general queueing networks, the problems become more complicated. A simple way to estimate the coefficient of variation of interarrival time (when the network is decomposable) is proposed. Besides the anomalies cited before, networks under certain topologies, such as networks with feedback loops, especially self loops, can not be decomposed into separate single servers when the coefficient of variation of service time distributions become large, even if the large variations are due to a large number of short service times. Nevertheless, the decomposability of a network can be improved by replacing each server with a self loop by an equivalent server without a self loop. Finally, we consider the service center with a queue dependent service rate or arrival rate. Generalization to two server closed queueing networks where each server may have a self loop is also considered.

PASSAGE TIME DISTRIBUTIONS FOR A CLASS OF QUEUEING NETWORKS: CLOSED, OPEN, OR MIXED, WITH DIFFERENT CLASSES OF CUSTOMERS WITH APPLICATIONS TO COMPUTER SYSTEM MODELING

by Philip S. Yu

Ballistic Missile Defense
Systems Command Contract
DASG60-77-C-0073
Computer time at SLAC
TR No. 135
March 1977

ABSTRACT

Networks of queues are important models of multiprogrammed time-shared computer systems and computer communication networks. Although equilibrium state probabilities of a broad class of network models have been derived in the past, analytic or approximate solutions for response time distributions or more general passage time distributions are still open problems. In this paper we formulate the passage time problem as a "hitting time" or "first passage time" problem in a Markov system and derive the analytic solution to passage time distributions of closed queueing networks. Efficient numerical approximation is also proposed. The result for closed queueing networks is further extended to obtain approximate passage time distributions for open queueing networks. Finally, we employ the techniques derived in this paper to study the interfault time and response time distribution and density functions of multiprogrammed computer systems. The effects of program behavior, degree of multiprogramming, size of main memory, service time of paging devices and rate of file I/O requests on the shape of distribution functions and density functions have been examined.

PROGRAM BEHAVIOR AND
THE PERFORMANCE OF
INTERLEAVED MEMORIES
by B. Ramakrishna Rau

ERDA Contract
EY-76-S-03-0326-PA 39
Computer time at SLAC
TR No. 138
SU-326-P.39-22
May 1977

ABSTRACT

One of the major factors influencing the performance of an interleaved memory system is the behavior of the request sequence, but this is normally ignored. This report examines this issue. Using trace driven simulations it is shown that the commonly used assumption, that all requests are equally likely to be to any module, is not valid. The duality of memory interference with paging is noted and this suggests the use of the Least-Recently-Used Stack Model to model program behavior. Simulation shows that this model is quite successful. An accurate expression for the bandwidth is derived based upon this model.

PERFORMANCE ANALYSIS OF
COMPUTER COMMUNICATION
NETWORKS VIA RANDOM
ACCESS CHANNELS
by Philip S. Yu

Ballistic Missile Defense
Systems Command Contract
DASG60-77-C-0073
Computer time at SLAC
TR No. 137
April 1977

ABSTRACT

The field of computer communication networks has grown very rapidly in the past few years. One way to communicate is via multiple access broadcast channels. A new class of random access schemes referred to as the M_p-persistent CSMA scheme is proposed. It incorporates the nonpersistent CSMA scheme and 1-persistent CSMA scheme, both slotted and unslotted versions, as its special cases with $p = 0$ and 1, respectively. The performance of the M_p-persistent CSMA scheme under packet switching is analyzed and compared with other random access schemes. By dynamically adjusting p, the unslotted version can achieve better performance in both throughput and delay than the currently available unslotted CSMA schemes under packet switching. Furthermore, the performance of various random access schemes under message switching is analyzed and compared with that under packet switching. In both slotted and unslotted versions of the M_0-persistent CSMA scheme, the performance under message switching is superior to that under packet switching in the sense that not only the channel capacity is larger but also the average number of retransmissions per successful message under message switching is smaller than that per successful packet under packet switching. In dynamic reservation schemes, message switching leads to larger channel capacity. However, in both slotted and unslotted versions of the ALOHA scheme, the channel capacity is reduced when message switching is used instead of packet switching. This phenomenon may also happen in the M_p-persistent CSMA scheme as p deviates from 0 to 1 for certain distributions of message length. Hence, the performance under message switching may be superior to or inferior to that under packet switching depending upon the random access scheme being used and the distribution of message length (usually a large coefficient of variation of message length implies a large degradation of channel capacity in this case) for certain random access schemes. Nevertheless, for radio channels, message switching can achieve larger channel capacity if appropriate CSMA schemes are used. A mixed strategy which is a combination of message switching and packet switching is proposed to improve the

performance of a point to point computer communication network when its terminal access networks communicate via highly utilized radio channels.

PROPERTIES AND APPLICATIONS
OF THE LEAST-RECENTLY-USED
STACK MODEL

by B. Ramakrishna Rau

ERDA Contract
EY-76-S-03-0326-PA 39
Computer time at SLAC
TR No. 139
SU-326-P.39-25
May 1977

ABSTRACT

The Least-Recently-Used Stack Model (LRUSM) is known to be a good model of temporal locality. Yet, little analysis of this model has been performed and documented. Certain properties of the LRUSM are developed here. In particular, the concept of the Stack Working Set is introduced and expressions are derived for the forward recurrence time to the next reference to a page, for the time that a page spends in a cache of a given size and for the time from last reference to the page being replaced. The fault stream out of a cache memory is modelled and it is shown how this can be used to partially analyze a multilevel memory hierarchy. In addition, the Set Associative Buffer is analyzed and a necessary and sufficient condition for the optimality of the LRU replacement algorithm is advanced.

ATMOSPHERIC PROBING
USING WAVE PROPAGATION MEASUREMENTS
by A. T. Waterman, Jr.
and R. W. Lee

NSF Grant ATM72-01407
Final Technical Report
June 1977

ABSTRACT

The objective of this research was the development of a technique for the remote measurement of wind and atmospheric turbulence. The technique involves the transmission of millimeter-length radio waves or of optical waves (or even of acoustic waves) between two locations in the atmosphere. By special modification and processing of the transmitted waves, the measurement is made sensitive to atmospheric conditions at just one point on the transmission path, and to just one scale size of atmospheric turbulence. Altering this modification of the waves leads to an alteration in the location of the sensitive point along the path, or to an alteration in the sensitive scale size. In this way, an examination of conditions along the path can be made; for example, one could measure a profile of the wind (actually the transverse component of the wind) along a line between two spaced points. The technique falls in the category of remote probing since no instruments are placed at the point where the measurement is made. As an example, the wind over an airport runway can be measured by placing the transmitting and receiving points well to either side of the runway.

The crux of the technique lies in the particular modification and processing of the transmitted waves. It is the use of spatial filters. In their crudest form, spatial filters may be no more than gratings. Two variants of the technique were made the subject of this research. In one, a spatial filter was used at the receiving end of the path only, and was supplemented by a variable temporal filter. In the second, spatial filters were used at both transmitting and receiving ends of the path. The first of these was applied to a path 28 km in length using 35 GHz radio waves (of 8.6 millimeter wavelength), since equipment which could be used for this purpose had been constructed and set up under a previous research program. The second was applied to shorter paths, ranging from 40 to 225 meters, and used incoherent optical waves (visible light from an incandescent bulb).

Successful operation of the technique was clearly demonstrated. Wind measurements obtained using the optical, double-spatial-filter approach

were checked against anemometer readings. The longer-path-length, millimeter-wave approach also was successful, though less easy to verify. Attempts to operate the optical equipment on a vertical path on San Francisco's Mt. Sutro Tower were less than satisfactory, being hampered by intense interference from the commercial TV and FM transmitters on the tower. Other proposed extensions of the technique could not be pursued owing to funding limitations. However, the experimental and measurements program was supplemented by a rather thorough theoretical analysis of the technique.

INTERPRETIVE MACHINES
by John K. Iliffe

JSEP Contract
N00014-75-C-0601
Course at Swansea
TR No. 149
June 1977

ABSTRACT

These lectures survey attempts to apply computers directly to high level languages using microprogrammed interpreters. The motivation for such work is to achieve language implementations that are more effective in some measure of translation, execution or response to the user than would otherwise be obtained. The implied comparison is with the established technique of compiling into a fixed general-purpose machine code prior to execution. It is argued that while substantial benefits can be expected from microprogramming it does not represent the best approach to design when the contributing factors are analysed in a general system context, that is to say when wide performance range, multiple source language, and stringent security requirements have to be satisfied. An alternative is suggested, using a combination of interpretation and a primitive instruction set and providing security at the microprogram level.

COMPUTING IN STORE
by John K. Iliffe

JSEP Contract
N00014-75-C-0601
TN No. 117
June 1977

ABSTRACT

These notes provide an introduction to the class of single-instruction, multiple-data stream computers with the simplest processing elements. Design principles are explained in terms of hypothetical Distributed Processor Arrays, with examples drawn from experimental systems. Emphasis is placed on (a) minimizing the cost differential when the DPA is compared with conventional main storage, and (b) designing the array control unit to support advanced forms of protection and language implementation. The influence of the DPA on general system design is examined briefly.

AD-A049 846 STANFORD UNIV CALIF STANFORD ELECTRONICS LABS F/G 9/2
SEMI-ANNUAL STATUS REPORT NUMBER 132, 1 JANUARY THROUGH 30 JUNE--ETC(U)
JUN 77 N00014-75-C-0601
UNCLASSIFIED SU-SEL-77-037 NL

2 of 2
ADA049 846

END
DATE FILMED
3-78
DDC

BROADCAST PROTOCOLS
IN PACKET SWITCHED
COMPUTER NETWORKS
by Yogen K. Dalal

DARPA, ARPA Order No. 2494
Contract MDA903-76-0093
NSF Grant MCS73-07973-A1,2
TR No. 128
April 1977

ABSTRACT

This thesis investigates the design and analysis of broadcast routing algorithms for use in store-and-forward packet switched computer networks. Broadcast routing is taken here to be a special case of multi-destination routing, in which a packet is delivered to all destinations rather than to some subset.

We examine five alternatives to transmitting separately addressed packets from the source to the destinations. The algorithms are compared qualitatively in terms of memory requirements, ease of implementation, adaptiveness to changing network conditions, and reliability. The algorithms are also compared quantitatively in terms of the number of packet copies generated to perform broadcast and the delays to propagate the packet to all destinations. Lower bounds on the performance measures are determined for all the algorithms by examining regular graphs.

Protocols that provide reliable communication using broadcast routing, i.e., broadcast protocols, are analogous to interprocess communication protocols except that communication is between one process and many processes. Reliable broadcast protocol design is faced with problems similar to those in the design of interprocess communication protocols - addressing, sequencing, duplicate detection and guarantee of delivery. This area presents many subjects for future research.

We describe a few applications for broadcast protocols in distributed computing environments. In particular, we show in detail how the catalog of a distributed file system could be structured in a simple way, if the system could make use of efficient reliable broadcast protocols.

The properties of reliable broadcast protocols at the host level emerge from the reliability of the routing algorithms and the applications for the protocols. We have examined the tradeoffs between global and subgroup broadcast routing. One conclusion we offer is that communication subnets should support both capabilities in the form of multi-destination addressing and reverse path forwarding, respectively.

An outcome of the investigation of broadcast routing algorithms is the formulation of two distributed (parallel) algorithms for constructing

minimal spanning trees. We believe that these algorithms are the first of their kind. The formulation of such algorithms has made the problems affecting the design of distributed algorithms in network environments clearer. These minimal spanning tree algorithms can be used in broadcast routing, as well as other networks like the Packet Radio Network.

SPRINT - AN INTERACTIVE
SYSTEM FOR PRINTED CIRCUIT
BOARD DESIGN USER'S GUIDE
by W. M. vanCleemput,
T. C. Bennett, J. A. Hupp,
and K. R. Stevens

ERDA Contract
E4-76-C-03-0515
and JSEP Contract
N00014-75-C-0601
TR No. 143
June 1977

ABSTRACT

The SPRINT system for the design of printed circuit boards is a collection of programs that allows designers to interactively design two-sided boards using a Tektronix 4013 graphics terminal. The major parts of the system are: a compiler for SDL, the Structural Design Language, an interactive component placement program, an interactive manual conductor routing program, an automatic batch router, a via elimination program and a set of artwork generation programs.

OXIDATION AND EPITAXY
by R. W. Dutton, D. A. Antoniadis, J. D. Meindl, T. I. Kamins, K. C. Saraswat, B. E. Deal, and J. D. Plummer

DARPA Contract
DAA-B07-75-C-1344
TR No. 5021-1
May 1977

ABSTRACT

The first order process models for silicon epitaxy and oxidation are described. Epitaxial dopant inclusion, autodoping and transient effects are discussed, and experimental results are presented. Silicon orientation, surface doping, and ambient effects are considered for silicon-oxidation rates.

STATISTICAL MODELING
by R. W. Dutton and
Dileep A. Divekar

DARPA Contract
DAA-B07-75-C-1344
Initial support through
H-P Corporate Eng.
TR No. 5021-2
May 1977

ABSTRACT

The Gummel-Poon model is reviewed with emphasis directed toward automated measurement. An algorithm for model parameter extraction is given and measured and simulated results are compared. A statistical sample of area-scaled transistors across a wafer has been characterized. Factor Analysis is used to help reduce the data and define a statistical model. Computer programs for Process and Device Simulation are used to facilitate understanding of the observed statistical variations and parameter correlations.

UNCLASSIFIED

SECURITY CLASSIFICATION OF THIS PAGE (When Data Entered)

REPORT DOCUMENTATION PAGE		READ INSTRUCTIONS BEFORE COMPLETING FORM
1. REPORT NUMBER 132	2. GOVT ACCESSION NO.	3. RECIPIENT'S CATALOG NUMBER
4. TITLE (and Subtitle) SEMI-ANNUAL STATUS REPORT NO. 132		5. TYPE OF REPORT & PERIOD COVERED Semi-Annual Status Report 1 Jan through 30 Jun 1977
		6. PERFORMING ORG. REPORT NUMBER SEL-77-037
7. AUTHOR(s) Information Systems, Digital Systems, Integrated Circuits, Solid-State Electronics, Radioscience, Ginzton Laboratory, and Inst. for Plasma Research		8. CONTRACT OR GRANT NUMBER(s) N00014-75-C-0601
9. PERFORMING ORGANIZATION NAME AND ADDRESS Stanford Electronics Laboratories Stanford University Stanford, California 94305		10. PROGRAM ELEMENT, PROJECT, TASK AREA & WORK UNIT NUMBERS
11. CONTROLLING OFFICE NAME AND ADDRESS U.S. Navy Office of Naval Research		12. REPORT DATE None 13. NO. OF PAGES 100
14. MONITORING AGENCY NAME & ADDRESS (if diff. from Controlling Office)		15. SECURITY CLASS. (of this report) Unclassified 15a. DECLASSIFICATION/DOWNGRADING SCHEDULE

16. DISTRIBUTION STATEMENT (of this report)

This document has been approved for public release and sale; its distribution is unlimited. Reproduction in whole or in part is permitted for any purpose of the United States Government.

17. DISTRIBUTION STATEMENT (of the abstract entered in Block 20, if different from report)

18. SUPPLEMENTARY NOTES

19. KEY WORDS (Continue on reverse side if necessary and identify by block number)

PLASMA PHYSICS, QUANTUM ELECTRONICS, RADIOSCIENCE, SOLID-STATE ELECTRONICS, SYSTEMS THEORY, DIGITAL SYSTEMS, INFORMATION SYSTEMS

20. ABSTRACT (Continue on reverse side if necessary and identify by block number)

The progress of research under each of the locally established project numbers for this contract is summarized.

DD FORM 1 JAN 73 1473

EDITION OF 1 NOV 65 IS OBSOLETE

UNCLASSIFIED

SECURITY CLASSIFICATION OF THIS PAGE (When Data Entered)

JSEP REPORTS DISTRIBUTION LIST

Department of Defense

Director
National Security Agency
Attn: Dr. T. J. Beahn
Fort George G. Meade, MD 20755

Defense Documentation Center (12)
Attn: DDC-TCA (Mrs. V. Caponio)
Cameron Station
Alexandria, VA 22314

Assistant Director
Electronics and Computer Sciences
Office of Director of Defense
Research and Engineering
The Pentagon
Washington, D.C. 20315

Defense Advanced Research
Projects Agency
Attn: (Dr. R. Reynolds)
1400 Wilson Boulevard
Arlington, VA 22209

Department of the Army

Commandant
US Army Air Defense School
Attn: ATSAD-T-CSM
Fort Bliss, TX 79916

Commander
US Army Armament R&D Command
Attn: DRSAR-RD
Dover, NJ 07801

Commander
US Army Ballistics Research Lab.
Attn: DRXRD-BAD
Aberdeen Proving Ground
Aberdeen, MD 21005

Commandant
US Army Command and
General Staff College
Attn: Acquisitions, Library Div.
Fort Leavenworth, KS 66027

Commander
US Army Communication Command
Attn: CC-OPS-PD
Fort Huachuca, AZ 85613

Commander
US Army Materials and
Mechanics Research Center
Attn: Chief, Materials Sci. Div.
Watertown, MA 02172

Commander
US Army Materiel Development
and Readiness Command
Attn: Technical Lib., Rm. 7S 35
5001 Eisenhower Avenue
Alexandria, VA 22333

Commander
US Army Missile R&D Command
Attn: Chief, Document Section
Redstone Arsenal, AL 35809

Commander
US Army Satellite Communications
Agency
Fort Monmouth, NJ 07703

Director
US Army Signals Warfare Laboratory
Attn: DELSW-OS
Arlington Hall Station
Arlington, VA 22212

Project Manager
ARTADS
EAI Building
West Long Branch, NJ 07764

NOTE: One (1) copy to each addressee unless otherwise indicated.

Commander/Director
Atmospheric Sciences Lab. (ECOM)
Attn: DRSEL-BL-DD
White Sands Missile Range, NM 88002

Commander
US Army Electronics Command
Attn: DRSEL-NL-O
(Dr. H. S. Bennett)
Fort Monmouth, NJ 07703

Director
TRI-TAC
Attn: TT-AD (Mrs. Briller)
Fort Monmouth, NJ 07703

Commander
US Army Electronics Command
Attn: DRSEL-CT-L (Dr. R. Buser)
Fort Monmouth, NJ 07703

Director
Electronic Warfare Lab. (ECOM)
Attn: DRSEL-WL-MY
White Sands Missile Range, NM 88002

Executive Secretary, TAC/JSEP
US Army Research Office
P. O. Box 12211
Research Triangle Park, NC 27709

Commander
Frankford Arsenal
Deputy Director
Pitman-Dunn Laboratory
Philadelphia, PA 19137

Project Manager
Ballistic Missile Defense
Program Office
Attn: DACS-DMP (Mr. A. Gold)
1300 Wilson Boulevard
Arlington, VA 22209

Commander
Harry Diamond Laboratories
Attn: Mr. John E. Rosenberg
2800 Powder Mill Road
Adelphi, MD 20783

HQDA (DAMA-ARZ-A)
Washington, D.C. 20310

Commander
US Army Electronics Command
Attn: DRSEL-TL-E (Dr. J.A. Kohn)
Fort Monmouth, NJ 07703

Commander
US Army Electronics Command
Attn: DRSEL-TL-EN
(Dr. S. Kroenenberg)
Fort Monmouth, NJ 07703

Commander
US Army Electronics Command
Attn: DRSEL-NL-T (Mr. R. Kulinyi)
Fort Monmouth, NJ 07703

Commander
US Army Electronics Command
Attn: DRSEL-NL-B (Dr. E. Lieblein)
Fort Monmouth, NJ 07703

Commander
US Army Electronics Command
Attn: DRSEL-TL-MM (Mr. N. Lipetz)
Fort Monmouth, NJ 07703

Commander
US Army Electronics Command
Attn: DRSEL-RD-O (Dr. W. S. McAfee)
Fort Monmouth, NJ 07703

Director
Night Vision Laboratory
Attn: DRSEL-NV-D
Fort Belvoir, VA 22060

Col. Robert Noce
Senior Standardization Representative
US Army Standardization Group, Canada
Canadian Force Headquarters
Ottawa, Ontario, Canada KIA)K2

Commander
US Army Electronics Command
Attn: DRSEL-NL-B (Dr. D.C. Pearce)
Fort Monmouth, NJ 07703

Commander
Picatinny Arsenal
Attn: SMUPA-TS-T-S
Dover, NJ 07801

Dr. Sidney Ross
Technical Director
SARFA-TD
Frankford Arsenal
Philadelphia, PA 19137

Commander
US Army Electronics Command
Attn: DRSEL-NL-RH-1
(Dr. F. Schwering)
Fort Monmouth, NJ 07703

Commander
US Army Electronics Command
Attn: DRSEL-TL-I
(Dr. C. G. Thornton)
Fort Monmouth, NJ 07703

US Army Research Office (3)
Attn: Library
P. O. Box 12211
Research Triangle Park, NC 27709

Director
Division of Neuropsychiatry
Walter Reed Army Institute
of Research
Washington, D.C. 20012

Commander
White Sands Missile Range
Attn: STEWS-ID-R
White Sands Missile Range, NM 88002

Department of the Air Force

Mr. Robert Barrett
RADC/ETS
Hanscom AFB, MA 01731

Dr. Carl E. Baum
AFWL (ES)
Kirtland AFB, NM 87117

Dr. E. Champagne
AFAL/DH
Wright-Patterson AFB, OH 45433

Dr. R. P. Dolan
RADC/ETSD
Hanscom AFB, MA 01731

Mr. W. Edwards
AFAL/TE
Wright-Patterson AFB, OH 45433

Professor R. E. Fontana
Head, Dept. of Electrical Engineering
AFIT/ENE
Wright-Patterson AFB, OH 45433

Dr. Alan Garscadden
AFAPL/POD
Wright-Patterson AFB, OH 45433

USAF European Office of
Aerospace Research
Attn: Major J. Gorrell
Box 14, FPO, New York 09510

LTC Richard J. Gowen
Department of Electrical Engineering
USAF Academy, CO 80840

Mr. Murray Kesselman (ISCA)
Rome Air Development Center
Griffiss AFB, NY 13441

Dr. G. Knausenberger
Air Force Member, TAC
Air Force Office of Scientific
Research, (AFSC) AFSOR/NE
Bolling Air Force Base, DC 20332

Dr. L. Kravitz
Air Force Member, TAC
Air Force Office of Scientific
Research, (AFSC) AFSOR/NE
Bolling Air Force Base, DC 20332

Mr. R. D. Larson
AFAL/DHR
Wright-Patterson AFB, OH 45433

Dr. Richard B. Mack
RADC/ETER
Hanscom AFB, MA 01731

Mr. John Mottsmith (MCIT)
HQ ESD (AFSC)
Hanscom AFB, MA 01731

Dr. Richard Picard
RADC/ETSL
Hanscom AFB, MA 01731

Dr. J. Ryles
Chief Scientist
AFAL/CA
Wright-Patterson AFB, OH 45433

Dr. Allan Schell
RADC/ETE
Hanscom AFB, MA 01731

Mr. H. E. Webb, Jr. (ISCP)
Rome Air Development Center
Griffiss AFB, NY 13441

LTC G. Wepfer
Air Force Office of Scientific
Research, (AFSC) AFOSR/NP
Bolling Air Force Base, DC 20332

LTC G. McKemie
Air Force Office of Scientific
Research, (AFSC) AFOSR/NM
Bolling Air Force Base, DC 20332

Department of the Navy

Dr. R. S. Allgaier
Naval Surface Weapons Center
Code WR-303
White Oak
Silver Spring, MD 20910

Naval Weapons Center
Attn: Code 5515, H. F. Blazek
China Lake, CA 93555

Dr. H. L. Blood
Technical Director
Naval Undersea Center
San Diego, CA 95152

Naval Research Laboratory
Attn: Code 5200, A. Brodzinsky
4555 Overlook Avenue, SW
Washington, D.C. 20375

Naval Research Laboratory
Attn: Code 7701, J. D. Brown
4555 Overlook Avenue, SW
Washington, D.C. 20375

Naval Research Laboratory
Attn: Code 5210, J. E. Davey
4555 Overlook Avenue, SW
Washington, D.C. 20375

Naval Research Laboratory
Attn: Code 5460/5410, J. R. Davis
4555 Overlook Avenue, SW
Washington, D.C. 20375

Naval Ocean Systems Center
Attn: Code 75, W. J. Dejka
271 Catalina Boulevard
San Diego, CA 92152

Naval Weapons Center
Attn: Code 601, F. C. Essig
China Lake, CA 93555

Naval Research Laboratory
Attn: Code 5510, W. L. Faust
4555 Overlook Avenue, SW
Washington, D.C. 20375

Naval Research Laboratory
Attn: Code 2627, Mrs. D. Folen
4555 Overlook Avenue, SW
Washington, D.C. 20375

Dr. Robert R. Fossum
Dean of Research
Naval Postgraduate School
Monterey, CA 93940

Dr. G. G. Gould
Technical Director
Naval Coastal System Laboratory
Panama City, FL 32401

Naval Ocean Systems Center
Attn: Code 7203, V. E. Hildebrand
271 Catalina Boulevard
San Diego, CA 92152

Naval Ocean Systems Center
Attn: Code 753, P. H. Johnson
271 Catalina Boulevard
San Diego, CA 92152

Donald E. Kirk
Professor and Chairman
Electronic Engineer, SP-304
Naval Postgraduate School
Monterey, CA 93940

Naval Air Development Center
Attn: Code 01, Dr. R. K. Lobb
Johnsville
Warminster, PA 18974

Naval Research Laboratory
Attn: Code 5270, B. D. McCombe
4555 Overlook Avenue, SW
Washington, D.C. 20375

Capt. R. B. Meeks
Naval Sea Systems Command
NC #3
2531 Jefferson Davis Highway
Arlington, VA 20362

Dr. H. J. Mueller
Naval Air Systems Command
Code 310
JP #1
1411 Jefferson Davis Highway
Arlington, VA 20360

Dr. J. H. Mills, Jr.
Naval Surface Weapons Center
Electronics Systems Department
Code DF
Dahlgren, VA 22448

Naval Ocean Systems Center
Attn: Code 702, H. T. Mortimer
271 Catalina Boulevard
San Diego, CA 92152

Naval Air Development Center
Attn: Technical Library
Johnsville
Warminster, PA 18974

Naval Ocean Systems Center
Attn: Technical Library
271 Catalina Boulevard
San Diego, CA 92152

Naval Research Laboratory
Underwater Sound Reference Division
Technical Library
P. O. Box 8337
Orlando, FL 32806

Naval Surface Weapons Center
Attn: Technical Library
Code DX-21
Dahlgren, VA 22448

Naval Surface Weapons Center
Attn: Technical Library
Building 1-330, Code WX-40
White Oak
Silver Spring, MD 20910

Naval Training Equipment Center
Attn: Technical Library
Orlando, FL 32813

Naval Undersea Center
Attn: Technical Library
San Diego, CA 92152

Naval Underwater Systems Center
Attn: Technical Library
Newport, RI 02840

Office of Naval Research
Electronic and Solid State
Sciences Program (Code 427)
800 North Quincy Street
Arlington, VA 22217

Office of Naval Research
Mathematics Program (Code 432)
800 North Quincy Street
Arlington, VA 22217

Office of Naval Research
Naval Systems Division
Code 220/221
800 North Quincy Street
Arlington, VA 22217

Director
Office of Naval Research
New York Area Office
715 Broadway, 5th Floor
New York, NY 10003

Office of Naval Research
San Francisco Area Office
One Hallidie Plaza, Suite 601
San Francisco, CA 94102

Director
Office of Naval Research
Branch Office
495 Summer Street
Boston, MA 02210

Director
Office of Naval Research
Branch Office
536 South Clark Street
Chicago, IL 60605

Director
Office of Naval Research
Branch Office
1030 East Green Street
Pasadena, CA 91101

Mr. H. R. Riedl
Naval Surface Weapons Center
Code WR-34
White Oak Laboratory
Silver Spring, MD 20910

Naval Air Development Center
Attn: Code 202, T. J. Shopple
Johnsville
Warminster, PA 18974

Naval Research Laboratory
Attn: Code 5403, J. E. Shore
4555 Overlook Avenue, SW
Washington, D.C. 20375

A. L. Slafkovsky
Scientific Advisor
Headquarters Marine Corps
MC-RD-1
Arlington Annex
Washington, D.C. 20380

Harris B. Stone
Office of Research, Development,
Test and Evaluation
NOP-987
The Pentagon, Room 5D760
Washington, D.C. 20350

Mr. L. Sumney
Naval Electronics Systems Command
Code 3042, NC #1
2511 Jefferson Davis Highway
Arlington, VA 20360

David W. Taylor
Naval Ship Research and
Development Center
Code 522.1
Bethesda, MD 20084

Naval Research Laboratory
Attn: Code 4105, Dr. S. Teitler
4555 Overlook Avenue, SW
Washington, D.C. 20375

Lt. Cdr. John Turner
NAVMAT 0343
CP #5, Room 1044
2211 Jefferson Davis Highway
Arlington, VA 20360

Naval Ocean Systems Center
Attn: Code 746, H. H. Wieder
271 Catalina Boulevard
San Diego, CA 92152

Dr. W. A. Von Winkle
Associate Technical Director
for Technology
Naval Underwater Systems Center
New London, CT 06320

Dr. Gernot M. R. Winkler
Director, Time Service
US Naval Observatory
Massachusetts Avenue at
34th Street, NW
Washington, D.C. 20390

Other Government Agencies

Dr. Howard W. Etzel
Deputy Director
Division of Materials Research
National Science Foundation
1800 G Street
Washington, D.C. 20550

Mr. J. C. French
National Bureau of Standards
Electronics Technology Division
Washington, D.C. 20234

Dr. Jay Harris
Program Director
Devices and Waves Program
National Science Foundation
1800 G Street
Washington, D.C. 20550

Los Alamos Scientific Laboratory
Attn: Reports Library
P. O. Box 1663
Los Alamos, NM 87544

Dr. Dean Mitchell
Program Director
Solid-State Physics
Division of Materials Research
National Science Foundation
1800 G Street
Washington, D.C. 20550

Mr. F. C. Schwenk, RD-T
National Aeronautics and
Space Administration
Washington, D.C. 20546

M. Zane Thornton
Deputy Director, Institute for
Computer Sciences and Technology
National Bureau of Standards
Washington, D.C. 20234

Nongovernment Agencies

Director
Columbia Radiation Laboratory
Columbia University
538 West 120th Street
New York, NY 10027

Director
Coordinated Science Laboratory
University of Illinois
Urbana, IL 61801

Director of Laboratories
Division of Engineering and
Applied Physics
Harvard University
Pierce Hall
Cambridge, MA 02138

Director
Electronics Research Center
The University of Texas
Engineering-Science Bldg. 112
Austin, TX 78712

Director
Electronics Research Laboratory
University of California
Berkeley, CA 94720

Director
Electronics Sciences Laboratory
University of Southern California
Los Angeles, CA 90007

Director
Microwave Research Institute
Polytechnic Institute of New York
333 Jay Street
Brooklyn, NY 11201

Director
Research Laboratory of Electronics
Massachusetts Institute of Technology
Cambridge, MA 02139

Director
Stanford Electronics Laboratory
Stanford University
Stanford, CA 94305

Stanford Ginzton Laboratory
Stanford University
Stanford, CA 94305

Officer in Charge
Carderock Laboratory
Code 18 - G. H. Gleissner
David Taylor Naval Ship Research
and Development Center
Bethesda, MD 20084

Dr. Roy F. Potter
3868 Talbot Street
San Diego, CA 92106